Results in Engineering 27 (2025) 106196

Contents lists available at ScienceDirect

Results in Engineering

journal homepage: www.sciencedirect.com/journal/results-in-engineering

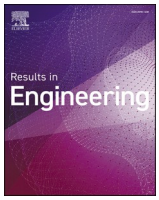

Experimental insights into injection timing effects upon VCR diesel engine fuelled with injected waste cooking oil ethyl ester-diesel blends and induced biogas operated in dual fuel mode

Prasant Kumar Patra [a], Swarup Kumar Nayak [a,b,*], Purna Chandra Mishra [a,*], Ganesan Subbiah [c], Nandagopal Kaliappan [d,e,*], Kamakshi Priya [f]

[a] School of Mechanical Engineering, Kalinga Institute of Industrial Technology (Deemed to be University), Odisha 751024, India
[b] School of Chemical Engineering, Kalinga Institute of Industrial Technology (Deemed to be University), Odisha 751024, India
[c] Department of Mechanical Engineering, Sathabama Institute of Science and Technology, Chennai, Tamil Nadu, India
[d] Department of Mechanical Engineering, Haramaya University, Harar, Ethiopia
[e] Department of Food Technology, Dhanalakshmi Srinivasan College of Engineering, Coimbatore, Tamil Nadu, India
[f] Department of Physics, Saveetha School of Engineering, Saveetha Institute of Medical and Technical Sciences (SIMATS), Saveetha University, Tamil Nadu, Chennai, India

A R T I C L E I N F O

Keywords:
Waste cooking oil ethyl ester
Biogas
Dual fuel mode (DFM)
Injection timing (IT)
Greenhouse gas
Waste-to-energy

A B S T R A C T

This study investigates the dual-fuel operation of a single-cylinder, four-stroke, 5.2 kW variable compression ratio (VCR) diesel engine fueled with a 20 % blend of waste cooking oil ethyl ester (WCOEE_20) and diesel as pilot fuel, and biogas (1.2 kg/h) as the inducted secondary fuel. The study aims to integrate renewable fuels into conventional diesel engines, promoting both efficiency and sustainability. Biogas was introduced through the intake manifold, while WCOEE_20 was directly injected into the combustion chamber. Experiments were performed at 1500 rpm and a compression ratio of 17.5:1, across varied injection timings (21°, 23°, 25°, and 27 °CA bTDC) to identify the optimal operating condition for enhanced combustion, performance, and emission behavior. Among all test cases, WCOEE_20+DFM25 °CA exhibited the best performance with a brake thermal efficiency (BTE) of 27.55 %—an improvement of 10.51 % over WCOEE_20+DFM23°, while 7.61 % lower than diesel operated in natural aspirated mode. This configuration reduced brake specific fuel consumption (BSFC) by 15.33 %, and exhaust gas temperature (EGT) increased by 3.28 %, compared to WCOEE_20+DFM23° while, 34.77 % increase in BSFC and 2.24 % decrease in EGT observed for plain diesel, respectively. Emission analysis showed reductions in CO (15.79 %), HC (16.0 %), NOx (17.41 %), and smoke opacity (28.49 %) relative to diesel fuel. Compared to WCOEE_20+DFM23°, smoke opacity decreased by 5.52 %, while NOx increased slightly by 9.67 %. Combustion analysis revealed that WCOEE_20+DFM25° caused a 0.83 % and 2.27 % increase in ignition delay period (IDP) over diesel and WCOEE_20+DFM23°, respectively, and combustion duration (CD) increased by 6.97 % and decreased by 2.76 %. Heat release rate (HRR) and cylinder pressure (CP) were found to be 3.58 % and 13.22 % higher than WCOEE_20+DFM23°, while 1.88 % lower and 10.02 % higher than normal diesel fuel in natural mode of aspiration. These findings demonstrate the potential of WCOEE_20+DFM25° as a cleaner and efficient alternative for diesel engine operation, supporting the United Nations Sustainable Development Goals (SDG) 7 (Affordable and Clean Energy) and SDG 13 (Climate Action).

Abbreviations: WCO, Waste cooking oil; WCOEE, Waste cooking oil ethyl ester; WCOEE_20, 20 % waste cooking oil ethyl ester; DFM, Dual fuel mode; IT, Injection timing; DI, Direct injection; VCR, Variable compression ratio; CR, Compression ratio; BTE, Brake thermal efficiency; BSFC, Brake specific fuel consumption; EGT, Exhaust gas temperature; CD, Combustion duration; IDP, Ignition delay period; HRR, Heat release rate; LHV, Lower heating value; NDIR, Non-dispersive infrared; C_v, Specific heat at constant vol.; DAQ, Data acquisition system; CA, Crank angle; NH_3, Ammonia; GWP, Global warming potential; A/F, Air/fuel ratio; CO, Carbon monoxide; HC, Hydrocarbon; NOx, Oxides of nitrogen; Smoke opacity, Exhaust smoke emission; CH_4, Methane; CO_2, Carbon dioxide; bTDC, Before top dead center; SDG, Sustainable Development Goal; SDG7, Sustainable Development Goal - Affordable and clean energy; SDG13, Sustainable Development Goal - Climate action; IOP, Injector opening pressure; ASTM, American society for testing and materials; B.gas, Biogas; SCO, Start of combustion; C_p, Specific heat at constant pressure; H_2S, Hydrogen sulfide; N_2O, Nitrous oxide; CNG, Compressed natural gas; aBDC, After bottom dead center.

* Corresponding authors.
E-mail addresses: swarup.nayakfme@kiit.ac.in (S.K. Nayak), pcmishrafme@kiit.ac.in (P.C. Mishra), nand204@gmail.com (N. Kaliappan).

https://doi.org/10.1016/j.rineng.2025.106196
Received 30 April 2025; Received in revised form 25 June 2025; Accepted 8 July 2025
Available online 11 July 2025

1. Introduction

Global energy sector is being significantly impacted by the quick decline of oil and gas reserves, rising costs of fuel, alongside increasing concern about harmful emissions. Petroleum-based energy sources that have driven economic development for more than a century are conventional and generate significant greenhouse pollutants, particularly carbon dioxide (CO_2), oxides of nitrogen (NO_x), and particulate matter (PM), that trigger global warming along with healthcare issues [1,2]. This development has encouraged scientists, researchers, legislators, and industries around the globe to increase their search for alternate, sustainable, as well as ecologically friendly energies. The increasing expense of traditional energies emphasizes the necessity of expanding energy resource assets using renewable sources [3]. With growing emphasis on wind and solar energy—technologies known for their carbon-neutral and renewable attributes—biodiesel has simultaneously gained interest as a liquid biofuel compatible with existing internal combustion engines [4]. Biodiesel sourced through a diverse range of bioenergy feedstocks—including agricultural trash, waste cooking oils, algae, alongside non-edible oil seeds—provide substantial benefits with regard to sustainability, decentralization, and compliance with presently employed diesel-powered vehicles [5,6]. Biomass-derived fuels offer a potential carbon-neutral or carbon-negative pathway, as the CO_2 emitted during combustion is approximately offset by that absorbed during biomass cultivation [7,8]. Furthermore, biomass reserves are generally common across suburban and rural places, providing energy access to dispersed and impoverished regions [9]. Alternative fuels, available in liquefied as well as gaseous forms, can provide viable options for the automotive and electricity-producing industries, assisting worldwide attempts to make the shift with regard to renewable energies, notably in accordance with SDGs 7 and 13 [10]. At present, several noticeable biomass-derived biodiesel are being thoroughly investigated to be potential substitute fuels over diesel-powered vehicles including alcohols, especially ethanol and methanol, noted for their elevated O_2 concentrations and clean-burning attributes; secondly, biodiesel produced from plant-based and animal-derived fats through transesterification process delivering a lesser greenhouse gases; alongside biogas, which is mainly comprised of methane, accomplished via anaerobic digestion of organic matter, offering a sustainable gaseous fuel which minimizes reliance upon petroleum-based natural gas while enhancing energy efficiency [11,12]. In most economically developed as well as developing nations, biodiesel mixing has emerged as an effective means to reducing dependency on petroleum and natural gas while lowering automobile exhaust pollutants. In recognition of its significant octane number as well as inexhaustible nature, ethanol has commonly mixed with liquid fuel in amounts that vary between 10–15 % (E10-E15), resulting in enhanced combustion performance and reduced carbon monoxide and hydrocarbon emissions [13,14]. In a comparable manner biodiesel, which is commonly mixed into petroleum-based fuel at a range of 5–10 % concentration (B5-B10), provides benefits including increased lubrication, sustainability, alongside lower pollutant emissions [15]. Biodiesel, made from sustainable organic materials like plant-based oils as well as animal-based fats, is known for its high biodegradability, non-toxicity, environmental compatibility, and low flammability rendering it an ideal substitute to traditional petroleum-based diesel. It has low sulfur concentration as well as oxygenated molecules, which contribute to better ignition and decreased levels of carbon monoxide, hydrocarbons, and particulates. Biodiesel is capable of being used in its purest state (BD100) or blended into different proportions with standard diesel (e.g., BD05, BD10, BD15, BD20 etc..) without requiring significant changes to existing diesel engine systems, fuel injection devices, or storage infrastructure—allowing for a smooth transition towards more sustainable energy sources [16,17]. Biogas, a sustainable energy source largely consisting of methane (CH_4 and CO_2), possesses a comparatively high octane value, often reaching 120. The high octane value indicates excellent resistance to spontaneous ignition and engine knocking making it particularly beneficial for diesel-powered vehicles with higher compression ratios [18]. In contradiction to low-octane energy sources, which typically pre-ignite during compression, biogas enables improved ignition timing alongside higher compression levels avoiding the possibility of knocking, allowing the combustion system to attain greater thermal performance. Increased thermal performance leads to better energy transformation towards productive mechanical work with lower brake specific fuel consumption (BSFC) [19]. Additionally, the ignition parameters of biogas are fundamentally different than those found in ordinary diesel. Being a lean-burn energy source, biogas assists in reducing ignition temperature, which helps to reduce the amount of nitrogen oxide (NOx) formation—one of the major emissions produced by diesel-powered vehicles. In the similar manner, consumption of biogas reduces emissions of smoke owing to its gaseous alongside oxygen-rich nature, so assisting in mitigating the classic NOx-smoke tradeoff which frequently confronts diesel vehicle pollution management [20,21]. Biogas is especially appropriate for diesel engines when employed as part of dual-fuel mode, in which a tiny amount of high-cetane fuel (e.g., diesel or biodiesel) serves as an initial source of combustion while biogas is supplied via the inlet manifold alongside ambient air. This dual-fuel technique necessitates only minor engine changes, usually restricted to changes within the inlet manifold that enable biogas infusion [22]. The diesel fuel provides consistent burning, whilst the injected biogas contributes to the primary ignition process, leading to less polluting and more efficient energy production. This combination enables biogas an appropriate replacement fuel for reducing greenhouse gas emissions in line with sustainable development along with ecological goals [23]. In a dual-fuel diesel engine, advancing the pilot injection timing increases the ignition delay period (IDP) because fuel is introduced through the combustion zone prematurely whilst both in-cylinder temperature as well as pressure are comparatively lower [24]. This prolonged premixed mixture stage enables for additional fuel-air blending, which results in an extremely intensive and quick burning when ignited. As a result, peak cylinder pressure (PCP) increases noticeably as more fuel ignites within a shorter period of time. This occurrence has a substantial impact on ignition behavior, improving thermal performance but possibly increasing NOx emissions due to higher in-cylinder temperatures [25]. Increasing IT in dual-fuel engines resulted in significant gains across engine efficiency, especially at minimal workload. At lesser loads, advancement of pilot fuel injection causes premature start of combustion (SOC), resulting in an extended premixed stage and improved air-fuel combination. This culminates into a more thorough and productive combustible process, which improves both brake thermal efficiency (BTE) alongside total ignition stability [26]. Increased combustion performance additionally serves to reduce carbon monoxide (CO) and unburned hydrocarbon (HC) pollutants by oxidizing additional fuel inside the combustion zone [27]. However, exceeding the optimal injection timing might cause a premature combustion of the pilot fuel when operating at more profound in-cylinder pressure along with reduced temperatures, particularly when performing at moderate as well as full-load conditions. This causes a substantial boost in the rate of pressure rise alongside peak cylinder pressures (PCP), that might result in knocking, accompanied by anomalous ignition noise and consequent wear and tear on the engine's components. Knocking not only reduces engine longevity; it also restricts the extent to which injection timing might be modified [27,28]. Furthermore, the synthesis of nitrogen oxides (NOx) rises during advancement in IT because of higher in-cylinder temperature alongside longer dwell time of combustion exhaust at higher temperatures, that promote thermal synthesis of NOx [29]. Advanced injection leads to elevated carbon dioxide (CO_2) outputs due to more efficient combustion completion. Although this is beneficial for thermal performance, it also means that the fuel's carbon content is converted into CO_2, a gas that causes global warming. As a result, there is a trade-off among maximizing efficiency while decreasing greenhouse gases, demanding precision injection timing optimization for balancing

efficiency, performance, and greenhouse gases [30]. Emitted smoke levels have been reported to be lower during advanced pilot injection timing because of improved premixed mixture of the fuel-air charge, that encourages more thorough burning thus reduces the generation of apparent smoke [31]. Meanwhile, as IT advanced, particulate matter (PM) outputs increased. This increase is mostly due to partial combustion produced by lower in-cylinder temperatures and pressures during the initial phases of the fuel injection process, which results in concentrated fuel-rich regions. Such circumstances encourage the clustering alongside coagulation of small fragments, increasing the amount of PM regardless of a noticeable drop in smoke opacity during advanced combustible settings [32,33].

1.1. Objective and novelty of the current work

Numerous studies have explored dual-fuel strategies using biodiesel and gaseous fuels. For instance, several investigations focused on biogas-diesel dual-fuel operation [34,35], while others examined biodiesel blends with natural gas or LPG [36,37]. However, most of these studies employed conventional diesel or edible-oil-based biodiesel as the pilot fuel and did not assess injection timing optimization in a variable compression ratio (VCR) engine, which adds an additional degree of freedom for performance enhancement and emissions control. Moreover, limited attention has been paid to the use of waste cooking oil ethyl ester (WCOEE)—a second-generation biofuel—in combination with biogas under precisely varied pilot fuel injection timings, particularly in VCR engine configurations. Existing literature either considers constant injection timing or fixed compression ratios, which constrains the full exploration of combustion dynamics under dual-fuel strategies. Furthermore, studies often lack a simultaneous evaluation of combustion, performance, and emissions characteristics with a quantitative comparative analysis across multiple injection timings, as conducted in current study. In the present investigation, a dual-fuel strategy was employed on a variable compression ratio (VCR) diesel engine to explore sustainable energy utilization by combining biogas with biofuel derived from waste cooking oil. Biogas was introduced through the inlet manifold as the primary inducted fuel, while the biofuel—produced via transesterification of waste cooking oil—was injected as a pilot fuel to initiate combustion. The VCR engine was modified to support dual-fuel operation, allowing precise control of the pilot fuel's injection timing (IT) to assess its impact on ignition characteristics. Injection timings were varied before top dead center (TDC) to identify the optimal setting for improving combustion efficiency. Key engine performance metrics, including brake thermal efficiency (BTE) and brake specific fuel consumption (BSFC), were evaluated under different load conditions. To further analyze combustion behavior across the range of ITs, ignition-related parameters such as in-cylinder pressure (CP), heat release rate (HRR), combustion duration (CD), and ignition delay period (IDP) were measured. Emissions of carbon monoxide (CO), unburnt hydrocarbons (HC), nitrogen oxides (NOx), and smoke opacity were also monitored and compared with those from standard diesel operation. The results revealed significant variations in engine performance under dual-fuel conditions, with certain injection timings enhancing thermal efficiency while reducing harmful emissions. This study underscores the potential of using biogas in combination with waste cooking oil ethyl ester as a viable alternative to conventional fossil fuels in VCR diesel engines, contributing to the goals of SDG 7 (Affordable and Clean Energy) and SDG 13 (Climate Action).

2. Material and methods

2.1. Waste cooking oil ethyl ester preparation and characterization

A base-catalyzed transesterification technique [7,38] has been employed to produce biofuel using waste cooking oil, a commonly available oil in local restaurants of Bhubaneswar. This method was executed utilizing a biodiesel reactor system housed in the building of KIIT (Deemed to be University) at Bhubaneswar, which has been designed for small-scale to medium-scale biofuel synthesis. In the transesterification reaction, waste cooking oil was combined alongside ethanol in the presence of a catalyst (potassium hydroxide), yielding ethyl ester biodiesel (WCOEE) and glycerol being the byproduct [39]. The resulting WCOEE constitutes a sustainable, renewable fuel featuring excellent combustible qualities, making it ideal for diesel-powered vehicles. The transesterification approach used in the present research complies alongside methodologies published in previous studies [40–42], resulting in significant yields and high-quality biofuel having minimal viscosity along with excellent combustion characteristics. The assessment of fuel samples is critical in determining their impact on engine efficiency, combustible characteristics, and exhaust properties.

Table 1 summarizes the key physicochemical characteristics of diesel and waste cooking oil ethyl ester (WCOEE), whereas Table 2 describes the gaseous composition and characteristics of biogas. Density, kinematic viscosity, flash point, fire point, calorific value, cetane number, pour point and carbon residue concentration are critical fuel factors that influence combustion performance and spray atomization in injected fuels. WCOEE, as a biofuel variant, exhibited higher specific gravity and kinematic viscosity over traditional diesel because of its inclusion on long-chain fatty acid ethyl esters [43,44]. The flash point of WCOEE was substantially greater, signifying increased safety while being handled or stored [45]. Despite WCOEE's lesser heating value in comparison to diesel implies a lesser energy content per unit mass, its inherent oxygen-rich structure promotes clean burning and decreases carbon-rich pollutants. Biogas, on the other hand, is distinguished for its significant methane concentration, relatively low density of energy, as well as elevated octane number, all of these contribute to its practicality to be the principal fuel for dual-fuel arrangements [46]. Biogas' toxic-free and zero-carbon nature emphasizes its significance in energy conservation systems, encouraging ecologically friendly engine efficiency in line with climate-resilient energy demands [47].

2.2. Biogas collection and characterization

Biogas employed in dual-fuel performance has been purchased commercially through Softex Industrial Products Pvt. Ltd. in Kolkata, West Bengal, India. A regulated inducement technique was implemented for supplying biogas, which is mostly made of methane along with carbon dioxide, inside the engine's inlet manifold [25,32]. The biogas functioned as the supplementary fuel, with WCOEE fueled straight inside the combustion chamber serving the test pilot fuel, resulting in a dual-fuel combustion approach. The integration of waste-to-energy transformation along with efficient ignition technique exemplifies a circular economy concept, which uses recyclable materials to produce renewable power. These initiatives not just minimize ecological damage triggered by waste cooking oil disposal, additionally they support Sustainable Development Goals (SDG) 7 and 13, which promote

Table 1
Key physio-chemical characteristics of conventional diesel fuel and waste cooking oil ethyl ester_100 and waste cooking oil ethyl ester_20 as per ASTM D-6751 standard.

Properties	Units	Diesel	WCOEE_100	WCOEE_20	ASTM D 6751
SG@15 °C	Kg/m^3	829.0	898.0	851.0	D 4052
KV@40 °C	CSt	2.54	3.71	2.82	D 445
LHV	MJ/kg	43.89	39.64	42.13	D 240
F_LP	°C	54.0	114.0	66.0	D 93
F_iP	°C	65.0	121.0	74.0	D 93
Pp	°C	−6.0	4.0	−4.0	D 97
CN	–	48.0	54.0	50.0	D 613
AcV	Mg KOH/g	0.05	0.37	0.14	D 974

** SG- Specific gravity; KV- Kinematic viscosity; LHV- Lower heating value; F_LP- Flash point; FiP- Fire point; Pp- Pour point; CN- Cetane number; AcV- Acid value.

Table 2
Gaseous composition and characteristics of biogas [22].

Properties	Biogas
Composition (by vol.)	CH_4- 67 %; CO_2. 31 %; H_2S (ppm)
Lower heating value (MJ/kg)	22.84
Specific gravity@15 °C (kg/m^3)	1.16
Octane number	120.0
Stoichiometric A/F ratio	9.6
Auto-ignition temperature (°C)	650.0
Flame speed (m/sec)	0.25
Boiling point (K)	112.0

accessibility to clean energy alongside mitigation of climate change via the use of carbon-free fuels.

2.3. Experimental setup and instrumentation

The test had been carried out on a single-cylinder, four-stroke, variable compression ratio (VCR), water-cooled, direct injection (DI) diesel engine positioned inside the I.C.Engine laboratory of Kalinga Institute of Industrial Technology (Deemed University), Bhubaneswar, Odisha, India. The diesel engine had been appropriately tailored to run in dual-fuel mode of operation, with waste cooking oil ethyl ester (WCOEE) as the pilot fuel and biogas as the major induced gaseous fuel. Fig. 1 depicts the testing setup's schematic arrangement, encompassing fuel delivery systems, gaseous fuel inducement methods, AVL 444 di-gas analyser, AVL 437-C smoke meter, and data acquisition systems for real-time performance and emissions assessment. Table 3 displays the precise technical details associated with the diesel-powered vehicle used in the current experiment. To simulate alongside modulate the load characteristics throughout experiments, an eddy current dynamometer was connected to the engine's output shaft. The dynamometer enabled for precision loading along with exact torque and speed monitoring across a variety of operational settings. This setup allowed a thorough examination of engine combustion, efficiency, and greenhouse gas characteristics for various fueling modes, injection timings, alongside loading conditions, resulting in reliable and accurate test outcomes. The engine's air inlet was accurately determined employing an air flow meter mounted above the inlet tube attached to the air surge tank, enabling a precise calculation of the volumetric air flow rate entering the combustion zone. The assessment is crucial for determining the fuel-air ratio, particularly in dual-fuel operations wherein biogas is introduced alongside inlet air. The storing balloon possessed a volumetric weight of 3 m^3 and comprised with robust synthetic rubber, thereby enabling gas impregnation alongside operational security. Biogas employed in dual-fuel performance has been purchased commercially through Softex Industrial Products Pvt. Ltd. in Kolkata, West Bengal, India, which had measurements of (3.04 m in length, 1.42 m in width, and 0.88 m in height). The storage facility provided a regulated plus continuous supply of biogas into the engine, allowing for equilibrium test operations while preserving uniform fuel mix and flow properties throughout dual-fuel modes of operation. The biogas retained inside the portable storage balloon was introduced into the engine's inlet manifold at a controlled pressure of 2.0 bar via a low-pressure, diaphragm-type gas compressor. This compressor provided a continuous and constant flow supply of biogas throughout engine operations, that's crucial in preserving steady combustibility in dual-fuel operation. The mass flow rate of biogas had been properly measured with a calibrated gas flow meter, enabling for precise fuel delivery regulation and subsequent evaluation across changing engine loading alongside operational settings. To make certain that biogas and intake air are mixed evenly before reaching the combustion zone, a Y-shaped gas-air mixing mechanism that functions analogous to a carburetor has been incorporated inside the engine's inlet manifold. This blending equipment improved the consistent dispersion of the biogas-air mixture, increasing its combustion performance and reducing cycle-to-cycle fluctuations. The configuration was intended to maximize the equivalency ratio while maintaining a uniform flame front throughout the combustion region. The engine's suction stroke causes a substantial pressure decrease within the venturi part of the inlet manifold which is caused by the rapid velocity of the fresh air flow. In accordance with Bernoulli's principle, a pressure drop is nearly equal to the square of the air entering the system. Since, the venturi's lower pressure zone produces a suction effect, facilitating biogas entrainment into the inlet air flow. This process assures that biogas is successfully extracted through the gas-air mixing unit alongside evenly mixed alongside the intake air, resulting in reliable and effective combustibility. A precise glass burette equipped with 2 optical fuel level indicators was used to properly measure the rate of ingestion of waste cooking oil ethyl ester (WCOEE) and diesel fuel throughout the combustion process.

These indicators enabled continuous assessment of gasoline use by measuring the fuel levels across two calibrated markings, allowing for accurate measurement of volumetric flow rates in the course of time. The above setup offered high-quality observations required for performance assessments over a variety of operational conditions alongside fuel mixtures. In-cylinder pressure (ICP) was determined employing a high-fidelity quartz piezoelectric pressure transducer. The detailed pressure readings allowed a thorough examination of combustion properties including ignition delay period (IDP), peak cylinder pressure (PCP), and combustion duration (CD), which are crucial for assessing fuel behavior and engine performance in dual-fuel operation. To record changing pressure differences throughout the combustion chamber, a high-precision piezoelectric pressure transducer had been flush-mounted onto the engine's head and directly connected alongside the clearance volume. This strategic positioning meant that ignition pressure indications were transmitted accurately, despite delay nor distortions. The transducer had been linked to a charge amplifier, that transformed the low-amplitude piezoelectric impulses onto quantifiable voltage output suited for high-fidelity combustible diagnosis. Such intensified inputs coordinated via the crankshaft's rotation to generate pressure-crank angle graphs, which allowed for accurate interpretations of combustion duration, ignition delay period, and peak pressure properties. A high-resolution crank angle encoder has been utilized to precisely link cylinder pressure readings alongside crankshaft rotation. This encoder had been attached straight with the engine's crankshaft alongside designed to produce signals at predetermined angular intervals, usually for each 0.8° of crankshaft rotation. During the in-cylinder ignition study, the piezoelectric pressure transducer alongside crank angle encoder were connected to a high-fidelity charge amplifier to accomplish a perfect alignment between pressure and crank angle measurements.

The augmented analog outputs were transmitted into a Data Acquisition System (DAQ), that encoded and recorded current information for every single crankshaft angle increase. This precise information was continually captured and saved onto a networked workstation for meticulous combustible diagnosis. For comprehending the thermodynamic characteristics of the combustible phenomenon, an additional combustion analyzer equipment has been employed. The above system used the pressure-crank angle measurements for determining essential combustion variables including heat release rate (HRR), start of combustion (SOC), and ignition delay period (IDP). These parameters enabled a thorough examination of energy release, ignition synchronization along with fuel-air reactions inside the combustion chamber yielding significant findings concerning dual-fuel operation. The engine's speed has been precisely determined employing a non-invasive optic device placed precisely proximal to the flywheel to track its rotary motion refrain from physical intrusion, resulting in exact and continuous speed monitoring. Three thermocouples of the K-type have been placed at significant locations to measure temperature parameters. One thermocouple has been placed inside the exhaust manifold to determine the exhaust gas temperature (EGT), providing information on combustion effectiveness as well as loss of heat. The second

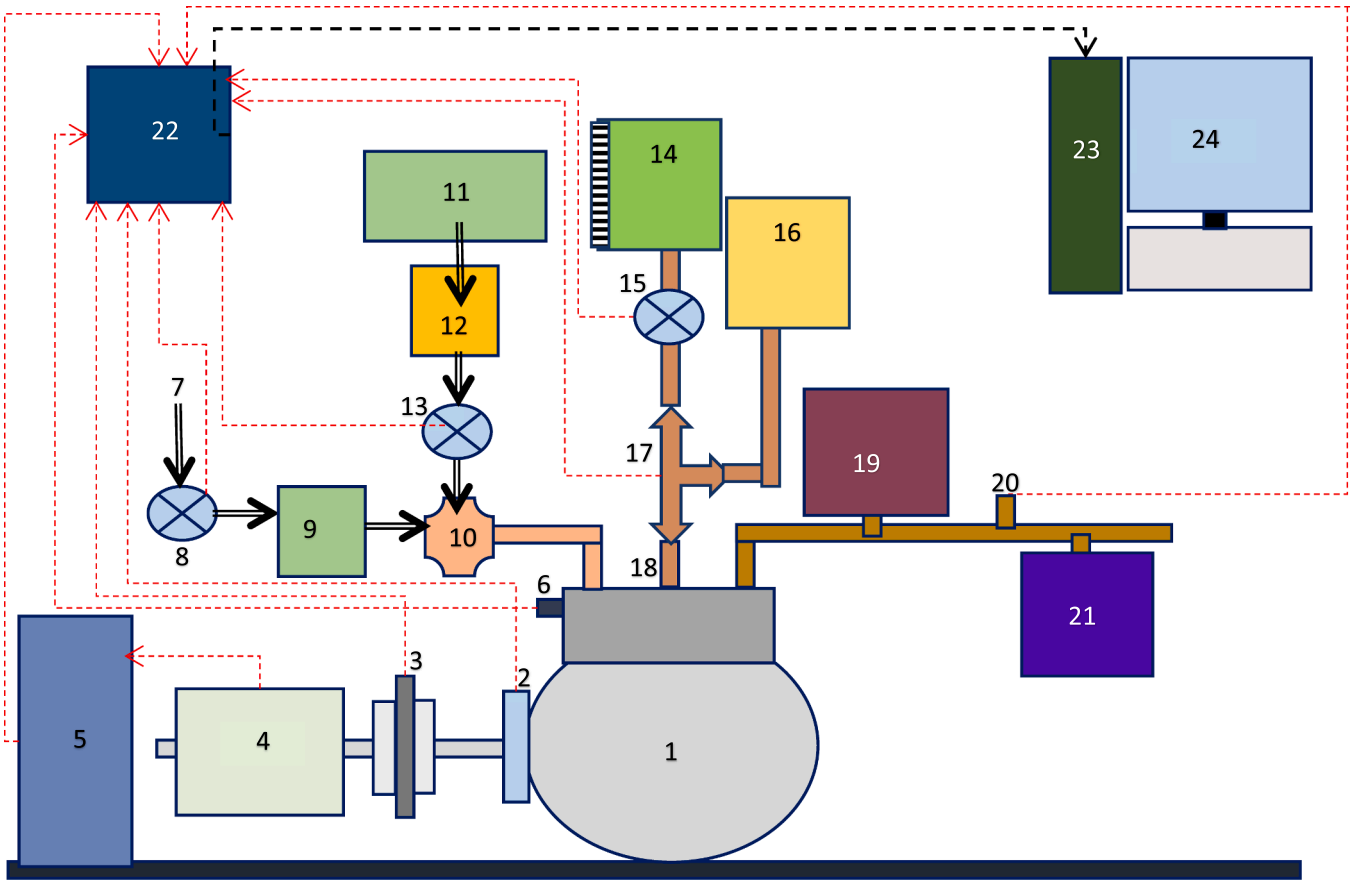

1. Engine
2. Crank angle encoder
3. Coupling
4. Eddy current dynamometer
5. Resistive load bank
6. Pressure transducer
7. Ambient air intake
8. Air flow meter
9. Air surge tank
10. Gas carburettor mixing kit
11. Biogas balloon
12. Biogas filtration unit
13. Biogas flow meter
14. Waste cooking oil ethyl ester tank
15. Fuel flow meter
16. Diesel tank
17. Solenoid valve
18. Fuel injector
19. AVL 444 di-gas analyser
20. K-type thermocouple
21. AVL 437-C smoke meter
22. Control pannel
23. Data acquisition system (DAQ)
24. Display unit (Computer system)

Fig. 1. Schematic layout diagram of the Test Rig.

thermocouple has been installed inside the inlet manifold to measure the temperature of the incoming air, and this affects air-fuel mixture along with volumetric efficiency. The third K-type thermocouple has been installed alongside the biogas delivery system to monitor the temperature of biogas delivered into the Y-shape gas carburetor, which is critical to comprehending combustion performance during various thermodynamic circumstances. A precise AVL 444 di-gas analyser has been employed to evaluate engine-generated greenhouse gases, including CO, HC, NOx, CO_2, and O_2, in accordance with ASTM D6751 standards. The exhaust emissions subsequently dehumidified alongside tested for CO, HC, and CO_2 measurements using a non-dispersive infrared (NDIR) detector. Each gas's thermal absorbing properties have been utilized to measure its content. NO emissions have been recorded utilizing an electrochemical sensor, that monitors the electrical charge produced

Table 3
Specification of the experimental setup.

Make/Model	Kirloskar TV1
Engine configuration	1-cylinder, 4-stroke, variable comperssion ratio, air cooled, direct injection diesel engine
Rated power	5.2 kW @ 1500 rpm
Speed	1500 rpm
Displacement volume	662 cm^3
Injection type	Direct injection
Stroke * Bore	110 mm * 87.5 mm
Injector opening pressure	210 bar
Injector timing	23°bTDC
Compression ratio	17.5:1

through the interaction of nitric oxide with a known solvent. This approach is highly sensitive, making it ideal for low-range NOx measurement. Smoke opacity, indicating particulate matter (PM) content, has been measured with a AVL 437-C smoke meter, that measures the intensity of light absorbed by soot fragments residing in fumes. Those extensive tests offer vital information upon combustion performance alongside greenhouse gas emissions across various fueling as well as injecting circumstances.

2.4. Experimental procedure and design of experiments (DOE)

To achieve precise engine efficiency as well as exhaust pollution characteristics assessment, the engine first operated until it attained the ideal temperature, resulting in a steady-state operation. This warming-up period considered crucial for reducing the impact of transient effects while stabilizing engine characteristics. When steady state had been established, baseline emission and ignition measurements were obtained employing traditional diesel alongside waste cooking oil ethyl ester (WCOEE) biofuels while operating in single-fuel configuration. Afterwards, the diesel engine switched towards dual-fuel operation through incorporating biogas to be the auxiliary induced gaseous fuel and keeping WCOEE-diesel blend being the pilot injection energy sources. The biogas was injected at a regulated flow rate of 1.21 kg/h across the inlet manifold to achieve moderate ignition, minimal knocking, along with improved thermal efficiency. Specifically, a calibrated gas flow meter was installed in the biogas supply line to measure the mass flow rate of biogas with high precision. The biogas was stored in a 3 m^3 high-strength rubberized storage balloon and was supplied to the engine via a low-pressure diaphragm-type gas compressor, which maintained a consistent supply pressure of 2.0 bar. This setup ensured that the biogas delivery remained stable throughout the test duration. Additionally, a Y-shaped gas-air carburettor mixer was used at the intake manifold to facilitate homogeneous mixing of biogas with ambient air before entering the combustion chamber, thus enhancing fuel-air uniformity and combustion stability. Throughout this period, the injector timing associated with the WCOEE pilot fuel mixture had been progressively changed at various crank angle positions to investigate the influence on start of combustion (SOC), ignition delay period (IDP), alongside total engine efficiency throughout dual-fuel operations. To ensure repeatability and reliability of results, each test point was replicated three times under identical environmental and operational conditions, and the average values were recorded. Care was taken to maintain consistent ambient temperature, fuel properties, and engine settings (load, speed, injection timing, etc.) throughout the experiments. Prior to every test, the engine was warmed up and stabilized to minimize the impact of transient conditions. Every experimental setting remained constant until accurate values for ignition pressure, heat expulsion, along with greenhouse gases had been obtained. This approach allowed for a thorough evaluation regarding the dual-fuel technique based on biogas-WCOEE, which contributed to a generation of greener and better performing energy-efficient diesel engines. To ensure steady engine functioning over changing load along with speed, throughout the examination, exact regulation for the WCOEE-diesel fuel flow rate seemed critical. The engine's integrated mechanical governor, essentially adjusts the amount of fuel injected in response to the engine's operating needs, was successfully used to accomplish this requirement. The governor ensured steady-state functioning during the examination by continually modifying the amount of WCOEE-diesel blended fuel, depending upon its speed and torque parameters. The injector timing was progressively changed in order to examine the pilot injection timing influencing ignition along with performance parameters. Steel shims with standard thickness were used to change the injector pump's mechanical configuration. The average thickness of every single shim utilized in the injector pump was 0.3 mm. An extra shim had been introduced for delaying the plunger's lifting power, which caused the time of injection to be prolonged by about 2° crank angle (°CA). On the other hand, the timing of the injection was advanced precisely through the same proportion when single shim was removed. This method made it possible to precisely and consistently modify the fuel injector scheduling, which made it possible to thoroughly examine the way that it affects the greenhouse gases, ignition delay period (IDP), combustion duration (CD), and heat release rate (HRR) for dual-fuel engines.

2.5. Uncertainty analysis

During experimentation, uncertainty assessment acts as a key method for determining the accuracy alongside precision of data collected. It's an important statistic for assessing the potential variations connected with assessment methods and estimated outcomes. In the absence of a quantifiable estimation of the uncertainty, the reliability as well as credibility associated with the acquired data becomes ambiguous, hindering the rigorous scientific methodology of the experiment. Uncertainty defines an interval in which the actual value associated with a recorded or calculated variable is anticipated to decrease alongside an anticipated level of confidence. In the current investigation, an uncertainty assessment has been conducted to determine the limits of accuracy over the engine-test outcomes. This research is especially important for comparing engine efficiency, combustibility, along with greenhouse gas emissions across different fueling sources including injecting techniques. The method used to estimate uncertainty is based on the approach suggested by Tiwari et al. [48], taking into account both systematic and random error during measurement. The conventional equation takes into account the specific uncertainty components of every equipment used in collecting information, as well as its sensitivity. Table 4 shows the computed uncertainty for every test equipment employed in this research, encompassing those that monitor fuel flow, air intake, cylinder pressure, exhaust gas composition, alongside temperature. Those defined uncertainty increase the reliability associated with outcomes of experiments and allow for more accurate analysis of the data patterns along with deviations.

$$U_{pp} = \sqrt{S_{pp}^2 + R_{pp}^2} \tag{2.5a}$$

Here, U_{pp} represents Uncertainty of physical parameters; S_{pp} and R_{pp} represents systematic uncertainty and random uncertainty correspondingly.+

$$\frac{S_{pp}}{pp} = \sqrt{\left[\sum_{i=1}^{n}\left(\frac{1}{pp}\frac{\partial pp}{\partial x_i}S_i\right)^2\right]} \tag{2.5b}$$

$$\frac{R_{pp}}{pp} = \sqrt{\left[\sum_{i=1}^{n}\left(\frac{1}{pp}\frac{\partial pp}{\partial x_i}R_i\right)^2\right]} \tag{2.5c}$$

Considering the circumstances of the present investigation's uncertainty assessment, the formula used to evaluate uncertainty originates using the universal principle of uncertainty propagation. According to

Table 4
Assessment of uncertainty over a wide range of testing equipment's.

Measured parameter	Instrument used	Range	Least count	Uncertainty (%)
Load (N)	Load cell	0–1000 N	±0.1 N	±0.2
Fuel flow rate (kg/sec)	Digital weighing balance	0–1 kg	±0.01 kg	±0.5
Air flow rate (kg/sec)	U-tube manometer	0–100 mm	±1.0 mm	±1.0
BP (kW)	Torque sensor & tachometer	0–10 kW	±0.01 kW	±0.3
EGT (°C)	K-type thermocouple	0–1200 °C	±1.0 °C	±0.75
CP (bar)	Piezoelectric pressure sensor	0–100 bar	±0.1 bar	±0.5
NO_x (ppm)	AVL 444 di-gas analyser	0–5000 ppm	±10.0 ppm	±1.0
CO (%)	AVL 444 di-gas analyser	0–10 %	±0.01 %	±1.2
HC (ppm)	AVL 444 di-gas analyser	0–10,000 ppm	±5.0 ppm	±1.4
Smoke Opacity (%)	AVL 437-C smoke meter	0–100 %	±1.0 %	±1.0
Instrument's overall uncertainty				±2.72 %

this composition, "pp" denotes a physical parameter being an outcome from one or more factors being measured as X_i. In the formula used to evaluate uncertainty, the physical parameter indicated with pp is regarded a dependent function of multiple independent experimental variables indicated by X_i. The overall uncertainty in the calculated component pp, represented as R_{pp}, is impacted by the degree of uncertainty associated with every reported variable, represented by R_i. These errors are due to limits in measuring devices, external factors, along with data acquisition system accuracy. The degree of uncertainty dissemination has been determined employing the root-sum-square approach, in which every component of uncertainty R_i has been squared then graded using its sensitivity coefficient (the partial derivative of pp with respect to X_i), after which all of these variables are added to give the total degree of uncertainty R_{pp}. For maximal statistical significance along with consistency, 25 different sets of measurements have been performed using very similar engine running circumstances, which include constant speed, load, as well as fuel properties. Repeated measurements enabled a more precise evaluation of systematic as well as random errors across each observed variables. The research investigative instruments alongside assessments had an overall uncertainty about

±2.72 %, demonstrating significant accuracy and reliability across the records. This validates the integrity of the research findings. The reliability studies were performed underneath similar circumstances to comprehensively investigate the uncertainty related to important operational alongside greenhouse gas characteristics. The variables including brake thermal efficiency (BTE), brake specific fuel consumption (BSFC), exhaust gas temperature (EGT), hydrocarbons (HC), carbon monoxide (CO), oxides of nitrogen (NOx), and smoke opacity had been separately investigated for uncertainty through reiterating every experiment five times in order to evaluate the results obtained. This reproducibility method enabled the detection and characterization of random errors in experiments as well as system operation. The standard deviation among the recorded data over repetitions has been used as a method of estimation for determining the variance, thereby determining the output's confidence range. This investigation considered instrument-specific uncertainties, ambient factors, including human oversight respectively. The overall uncertainty (Δ) of the experiment obtained as ±2.68 %:

$$\Delta = \sqrt{BTE^2 + BSFC^2 + EGT^2 + CO^2 + HC^2 + Smoke^2 + NOx^2 + IDP^2 + CD^2}$$

$$\Delta = \sqrt{0.65^2 + 1.5^2 + 1.0^2 + 1.0^2 + 0.5^2 + 0.8^2 + 1.0^2 + 0.8^2 + 0.5^2}$$
$$= \pm 2.68\%$$

3. Result and discussion

3.1. Performance analysis

Performance analysis in a diesel engine involves evaluating key parameters including brake thermal efficiency (BTE), brake specific fuel consumption (BSFC), and exhaust gas temperature (EGT) to understand the engine's energy conversion efficiency and operational effectiveness. BTE measure effectively the chemical energy of fuel converted into useful mechanical work. BSFC assesses the amount of fuel consumed per unit of power output. EGT provides insights into the thermal loading and combustion characteristics inside the cylinder.

3.1.1. Brake thermal efficiency

The Fig. 2 represent the variation of brake thermal efficiency (BTE) with brake power output for different fuel modes in a variable compression ratio diesel engine operating at a constant speed of 1500 rpm, injection pressure of 240 bar and a compression ratio of 17.5:1. BTE, a key indicator of how efficiently an engine converts the chemical energy of the fuel into useful mechanical work, is expressed as a percentage. Higher BTE value represent more efficient fuel utilization and combustion. The fuels tested include baseline diesel, WCOEE_20 (a 20 % blend of waste cooking oil ethyl ester with diesel), and other dual-fuel modes including (WCOEE_20+DFM21°; WCOEE_20+DFM23°; WCOEE_20+DFM25° and WCOEE_20+DFM27°) in which biogas is induced alongside WCOEE_20 at varying injector timing of 21°, 23°, 25°, and 27° bTDC, respectively. As brake power increases from 1.28 kW to 5.12 kW, BTE increases for all fuel types, which is typical behaviour in internal combustion engine due to improved combustion efficiency at higher loads [49]. At elevated loads, the increase in-cylinder temperature and pressure enhances the combustion of both the main and pilot fuels, thereby improving the thermal efficiency [50]. This trend is also reflected in the rise in exhaust gas temperature (EGT), which increases with load and correlates with better combustion and higher energy release [48]. Diesel consistently records the highest BTE across all power outputs, starting at 15.08 % at 1.28 kW and peaking at 29.82 % at 5.12 kW. This is attributed to diesel's superior combustion characteristics, high cetane number, and energy density, which facilitate more complete and efficient combustion [51,52]. WCOEE_20, though renewable and clean-burning, exhibits slightly lower BTE over diesel across all loads, ranging from 13.35 % at 1.28 kW to 27.15 % at 5.12 kW maximum loads. The reduction is due to the higher kinematic viscosity and oxygen content of biodiesel, which can result in poorer atomization, delayed combustion, and increased heat losses at lowest temperatures [53]. However, as the load increases, the efficiency gap between diesel and WCOEE_20 narrows, indicating that WCOEE_20 performs comparably well under optimal thermal conditions. In dual-fuel operational modes involving biogas induction, BTE is generally lower contrast to diesel and WCOEE_20 single-fuel modes, especially at lower brake powers. WCOEE_20+DFM21 records only 9.9 % BTE at 1.28 kW due to biogas's poor auto-ignition properties, low flame speed, and lower calorific value, which result in incomplete combustion under low load and temperature conditions. This is reflected in the lowest corresponding EGT of 147.65 °C, confirming sub-optimal heat release and unburnt fuel [54]. However, as brake power increases, BTE improves in all dual-fuel cases, confirming that higher loads provide better combustion environments even for low-reactivity fuels including biogas. Among the dual-fuel setups, WCOEE_20+DFM25° consistently shows higher BTE, rising from 13.2 % at 1.28 kW to 27.55 % at 5.12 kW. The peak EGT for this case is 362.42 °C, slightly lower than diesel but higher than other dual-fuel modes, suggesting efficient combustion with minimal

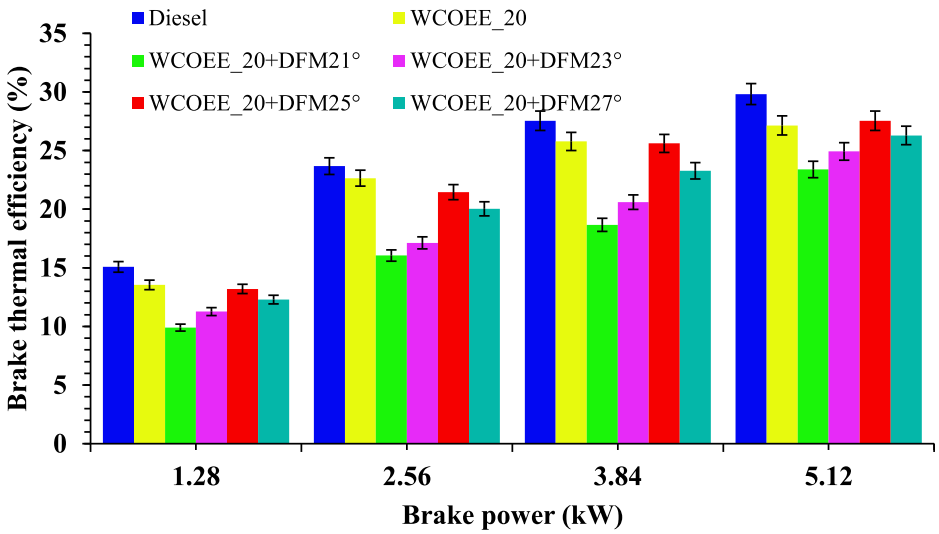

Fig. 2. Effect of test fuel blends with varying injector timing on BTE (%) vs. BP (kW).

post-combustion energy loss [29]. This advanced injection timing of 25° bTDC allows more time for air-fuel mixture and improves ignition conditions, resulting in more complete combustion. WCOEE_20+DFM27°,while also using advanced injection timing, shows slightly reduced efficiency at higher loads (26.29 % at 5.12 kW). Its EGT of 362.42 °C, higher than WCOEE_20+DFM25°, implies increased in-cylinder heat and earlier combustion phasing that may have resulted in elevated peak pressures before TDC, leading to mechanical losses and sub-optimal energy utilization [55]. Conversely, retarded injection (DFM21°) consistently shows lower BTE across all loads due to shortened ignition delay and poor mixing, which is supported by its relatively low EGT of 312.57 °C, indicating lower combustion efficiency [56]. Thus, the EGT trends affirm that WCOEE_20+DFM25° not only shows the highest BTE among the dual-fuel cases but also exhibits a thermally balanced combustion process, where sufficient ignition delay and controlled energy release lead to optimal combustion efficiency. Similar findings were reported by Yusuf et al. [57] supporting the consistency of present result. At peak load of 5.12 kW, BTE values for WCOEE_20; WCOEE_20+DFM21°; WCOEE_20+DFM23°; WCOEE_20+DFM25° and WCOEE_20+DFM27° are found to be 27.14 %, 23.39 %, 24.93 %, 27.55 %, and 26.29 % which are found to be 8.99 %, 21.56 %, 16.39 %, 7.61 %, and 11.83 % lower than diesel fuel (29.82 %) respectively.

3.1.2. *Brake specific fuel consumption*

The Fig. 3 illustrates the variation in brake specific fuel consumption (BSFC) for variable compression ratio diesel engine fuelled with different blends and modes, plotted against increasing brake power outputs of 1.28, 2.56, 3.84 and 5.12 kW respectively. BSFC is a measure of fuel efficiency, is expressed in g/kW.h and represents the amount of fuel required to produce one kilowatt of power in one hour. The experiment was conducted at a constant engine speed of 1500 rpm, injection pressure of 240 bar and compression ratio of 17.5:1. The fuel variants include, diesel, WCOEE_20 (a 20 % blend of waste cooking oil ethyl ester with diesel), and other dual-fuel modes including (WCOEE_20+DFM21°; WCOEE_20+DFM23°; WCOEE_20+DFM25° and WCOEE_20+DFM27°) in which biogas is induced alongside WCOEE_20 at varying injector timing of 21°, 23°, 25°, and 27° bTDC, respectively. The overall trend observed in the above figure is a constant decline in BSFC with increasing brake power for all prepared test fuel blends in both single and dual fuel mode of operation, which might be expected due to improved combustion efficiency at higher loads [58]. As the load increases, the combustion becomes more complete due to elevated in-cylinder temperature and

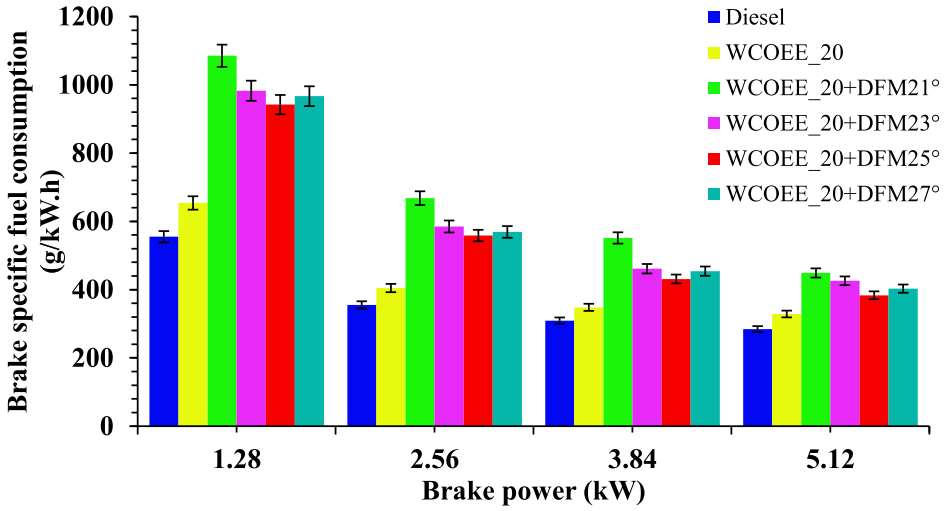

Fig. 3. Effect of test fuel blends with varying injector timing on BSFC (g/kW.h) vs. BP (kW).

pressure, thereby leading to improved atomization and fuel-air blending, which leads to more complete combustion. These effects are supported by rising exhaust gas temperature (EGT) values, which indicate higher post-combustion energy release [59]. Quantitatively, diesel exhibits the lowest BSFC values across all outputs- 554.93 g/kW.h at 1.28 kW, reducing to 284.54 g/kW.h at 5.12 kW- but also shows a corresponding increase in EGT from 172.58 °C at minimum load to 370.74 °C at full load, reflecting superior combustion quality and energy conversion efficiency highlighting its superior energy density and combustible characteristics [56]. In contrast, WCOEE_20 demonstrates a higher BSFC values at all loads, ranging from 653.9 g/kW.h at 1.28 kW to 328.72 g/kW.h at 5.12 kW. This increase is attributed to the lower heating value and higher kinematic viscosity of WCOEE_20 blend, which impairs its atomization and combustion efficiency [53,59]. The induction of biogas in dual-fuel operational mode significantly elevates BSFC across all workloads, with the most pronounced effect observed at lower brake power. For instance, at 1.28 kW, BSFC values reach 1085.13 g/kW.h; 982.66 g/kW.h for WCOEE_20+DFM21° and WCOEE_20+DFM23°, compared to 653.9 g/kW.h for WCOEE_20 alone. The rise in BSFC in dual-fuel modes of operation is primarily due to biogas's lower energy density and poor combustion characteristics under lower load conditions, resulting in incomplete ignition and higher fuel consumption [60]. Injection timing plays a vital role in optimizing BSFC in dual-fuel operations. Retarded injection timing (21° bTDC) results in highest BSFC values, indicating poor combustion efficiency due to reduced ignition delay and inadequate mixing-with an associated EGT of 147.65 °C at low load and 312.57 °C at peak load—indicative of sub-optimal combustion. Advancing the injection timing progressively to 23°, 25° and 27° bTDC improves combustion by allowing more time for air-fuel mixture before ignition, with a corresponding EGT increase from 175.14 °C to 366.26 °C, supporting the observed improvement in combustion efficiency—thereby reducing BSFC. At 5.12 kW, BSFC drops from 448.89 g/kW.h for (DFM21°) to 383.51 g/kW.h for (DFM25°), demonstrating the benefit of advanced injection timing. However, excessively advanced timing of (DFM27°) slightly increased BSFC (402.95 g/kW.h), likely due to premature ignition, increased heat losses, and reduced effective power output [61]. Thus, WCOEE_20+DFM25° shows the most favourable BSFC among the dual-fuel modes, particularly at higher loads, implying 25° bTDC as the best injection timing for biogas-inducted dual-fuel operation. These findings are in alignment with those reported by Prasad et al. [62], further emphasizing the potential of biodiesel-biogas dual-fuel systems. At peak load of 5.12 kW, BSFC values for WCOEE_20; WCOEE_20+DFM21°; WCOEE_20+DFM23°; WCOEE_20+DFM25° and WCOEE_20+DFM27° are found to be 328.72 g/kW.h; 448.89 g/kW.h; 425.92 g/kW.h; 383.51 g/kW.h and 402.95 g/kW.h which are found to be 15.53 %, 57.77 %, 49.68 %, 34.77 % and 41.63 % higher than diesel fuel (284.54 g/kW.h) respectively.

3.1.3. Exhaust gas temperature

The Fig. 4 elaborates the variation of exhaust gas temperature (EGT) with brake power output for all prepared fuel blends in a VCR diesel engine operated at constant speed of 1500 rpm, an injection pressure of 240 bar, and a compression ratio of 17.5:1. Exhaust gas temperature is a critical parameter in engine diagnostics and performance, analysis, as it reflects the thermal load on engine components and offers insights into combustion efficiency [63]. Generally, higher EGT indicates higher combustion temperatures, which can either imply improved combustion or, if excessively high, imply incomplete combustion or delayed heat release. In this investigation, 6 fuel modes are examines, diesel, WCOEE_20 (a 20 % blend of waste cooking oil ethyl ester with diesel), and other dual-fuel modes including (WCOEE_20+DFM21°; WCOEE_20+DFM23°; WCOEE_20+DFM25° and WCOEE_20+DFM27°) in which biogas is induced alongside WCOEE_20 at varying injector timing of 21°, 23°, 25°, and 27° bTDC, respectively. As brake power increases from 0 to 5.12 kW, the EGT consistently rises for all fuel modes, reflecting the increase in fuel supply and combustion heat release associated with higher engine loads. Diesel exhibits a gradual increment in EGT from 150.2 °C at idle (0 kW) to maximum of 370.7 °C at full load (5.12 kW). This trend reflects diesel's efficient combustion characteristics under increased loading conditions, where more fuel is injected and efficiently burned, leading to higher heat release [64]. WCOEE_20 shows slightly higher EGT across all loads compared to diesel fuel, ranging from 164.3 °C at idle to 409.7 °C at peak load. The elevated temperature range might be due to its inherent oxygen content, which promotes prolonged and more complete combustion, thus increasing in-cylinder temperature and leading to higher EGT [57]. Additionally, biodiesel's higher kinematic viscosity can cause delayed combustion, resulting in extended post-combustion heat release that might also contribute to higher EGT [65,66]. Among the dual fuel modes, WCOEE_20+DFM21° (retarded injection timing) consistently shows the lowest EGT values at all loads, from 128.5 °C at idle to 312.6 °C at maximum loading condition. This is primarily due to the retarded injection causing poor fuel-air mixing and delayed ignition, leading to incomplete combustion and lower peak combustion temperatures [67].

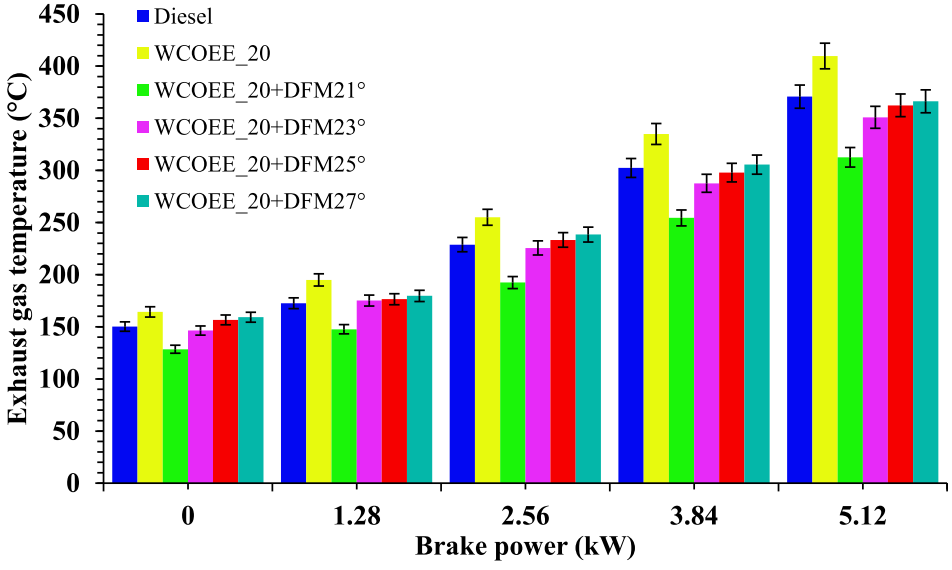

Fig. 4. Effect of test fuel blends with varying injector timing on EGT (°C) vs. BP (kW).

The limited reactivity of biogas also plays a role, as its low flame speed and high ignition delay contribute to lower in-cylinder temperatures and reduced heat transfer to exhaust gases. As injection timing advances to 23°, 25° and 27° bTDC, the EGT values progressively rises. WCOEE_20+DFM23° records EGTs from 146.4 °C at idle to 350.9 °C at maximum load, while WCOEE_20+DFM25° shows range of 156.6 °C to 350.9 °C, and WCOEE_20+DFM27° yields the highest EGT among dual-fuel configurations, from 159.2 °C at idle to 366.3 °C at peak loads. These increments can be attributed to enhanced combustion due to better air-fuel mixing and increased residence time before TDC, enabling more complete combustion and greater heat release within the engine cylinder, thereby increasing EGT [68,69]. Interestingly, while advancing injection timing improves combustion quality, and hence increases EGT, excessively advanced injector timing of 27° bTDC, may push combustion closer to the compression stroke, resulting in increased heat losses to cylinder walls and potentially reduced net work output despite higher temperatures. Nevertheless, these higher EGTs indicate more energetic combustion events, albeit with possible trade-offs in engine efficiency and thermal stresses. In general. The biogas-induced dual-fuel modes shows lower EGTs than pure WCOEE_20 in single fuel modes and diesel fuel at lower loads due to biogas's lower calorific value and reactivity. However, as load increases, the combustion environment becomes more favourable for biogas oxidation, and the EGT rises, especially when injection timing is optimized [70]. Similar findings were reported by Marikatti et al. [71] supporting the consistency of present result. At peak load of 5.12 kW, EGT values for WCOEE_20; WCOEE_20+DFM21°; WCOEE_20+DFM23°; WCOEE_20+DFM25° and WCOEE_20+DFM27° are found to be 409.73 °C, 312.57 °C, 350.92 °C, 362.43 °C, and 366.26 °C which are found to be 10.52 % higher while, 15.69 %, 5.35 %, 2.24 %, and 1.21 % lower than diesel fuel (370.74 °C) respectively.

3.2. Emission analysis

Emission analysis in a diesel engine focuses on measuring and understanding the levels of key pollutants including carbon monoxide (CO), unburnt hydrocarbon (HC), oxides of nitrogen (NOx) and smoke opacity. These emissions are crucial indicators of combustion quality, fuel efficiency, and environmental impact. CO and HC emissions primarily result from incomplete combustion, often caused by poor fuel-air mixing, insufficient temperature or rich fuel mixtures. NOx, emission on other hand, are formed by high combustion temperature and presence of excessive oxygen content, following thermal NOx formation mechanism. Smoke emission is the indicator of soot particles generated owing to partial combustion of fuel, especially in fuel-rich zones.

3.2.1. Carbon monoxide emission (CO)

The Fig. 5 presents the variation in carbon monoxide (CO) emissions in grams per kilowatt-hour (g/kW·h) as a function of brake power output for different fuel blends and dual-fuel combustion modes in a single-cylinder diesel engine operating at a constant speed of 1500 rpm, injection pressure of 240 bar, and compression ratio of 17.5:1. Carbon monoxide is a by-product of incomplete combustion and serves as an indicator of the combustion efficiency of the fuel-air mixture. The tested fuel modes include conventional diesel, WCOEE_20 (a 20 % blend of waste cooking oil ethyl ester with diesel), and four dual-fuel variants using WCOEE_20 and biogas with injection timings of 21°, 23°, 25°, and 27° before top dead center (bTDC), labeled as WCOEE_20+DFM21°, DFM23°, DFM25°, and DFM27° respectively. At the lowest load of 1.28 kW, CO emissions are at their highest for all fuel modes due to lower combustion temperatures and incomplete oxidation, which are typical under light load conditions [72]. Diesel registers a CO emission of 0.049 g/kW·h, while WCOEE_20 slightly improves the emission profile to 0.042 g/kW·h, indicating a marginally better oxidation capability likely due to the inherent oxygen content of the biodiesel blend. EGT values at this load further reinforce the trend: diesel reaches 172.58 °C and WCOEE_20 rises marginally to 194.96 °C, still insufficient for complete oxidation [59,63]. Among the dual-fuel combinations, WCOEE_20+DFM21° exhibits the highest CO emission at 0.053 g/kW·h, a result of retarded injection timing that causes delayed combustion and poor mixing, leading to incomplete fuel oxidation. The CO emissions for DFM23°, DFM25°, and DFM27° stand at 0.048, 0.044, and 0.046 g/kW·h respectively, reflecting the gradual improvement in combustion with more advanced injection timing that enhances air-fuel mixing and ignition readiness. As the brake power increases to 2.56 kW, a significant reduction in CO emissions is observed across all fuel modes, driven by improved combustion temperature and pressure conditions that facilitate more complete oxidation of carbon-based fuels [73]. Diesel records a CO emission of 0.023 g/kW·h, WCOEE_20 drops to 0.018 g/kW·h, while dual-fuel modes exhibit emissions in the range of 0.019 to 0.028 g/kW·h. Notably, WCOEE_20+DFM21° still shows higher emissions (0.028 g/kW·h) than its counterparts, reinforcing the negative impact of retarded injection timing on combustion completeness. On the other hand, WCOEE_20+DFM25° demonstrates improved performance (0.019 g/kW·h), suggesting that the advanced timing facilitates better thermal conversion of fuel energy. At intermediate and higher loads of 3.84 and 5.12 kW, CO emissions continue to decrease for most configurations, consistent with higher in-cylinder temperatures and improved reaction

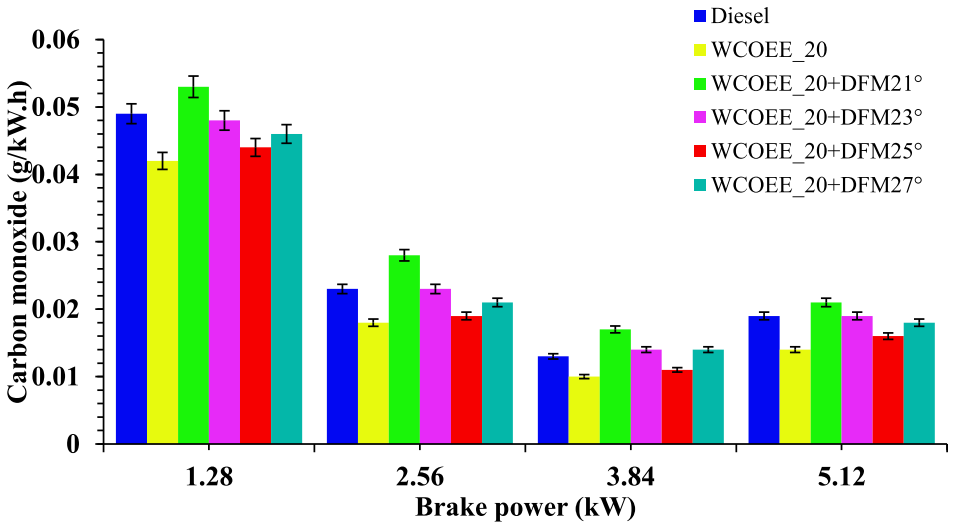

Fig. 5. Effect of test fuel blends with varying injector timing on CO (g/kW.h) vs. BP (kW).

kinetics that minimize the generation of CO [74,75]. At 3.84 kW, diesel and WCOEE_20 emit 0.013 and 0.01 g/kW·h respectively, while the dual-fuel configurations vary between 0.012 and 0.017 g/kW·h. Advanced timing modes such as DFM25° and DFM27° perform relatively better due to optimized combustion phasing, enabling more effective oxidation of carbon species before exhaust [76]. At full load (5.12 kW), the lowest CO emissions are recorded for WCOEE_20 (0.014 g/kW·h), followed closely by DFM25° (0.016 g/kW·h), DFM27° (0.018 g/kW·h), and diesel (0.019 g/kW·h). Interestingly, WCOEE_20+DFM23° and DFM21° still produce relatively higher CO emissions (0.021 and 0.02 g/kW·h, respectively), suggesting that combustion efficiency remains inferior in these cases due to either sub-optimal phasing (DFM23°) or overly delayed ignition (DFM21°). Thus, WCOEE_20+DFM25° shows the most favourable CO emission among the dual-fuel modes, particularly at higher loads, implying 25° bTDC as the best injection timing for biogas-inducted dual-fuel operation. These findings are consistent with the conclusion drawn by Reddy et al. [77], further emphasizing the potential of biodiesel-biogas dual-fuel systems. At peak load of 5.12 kW, CO emission values for WCOEE_20; WCOEE_20+DFM21°; WCOEE_20+DFM23°; WCOEE_20+DFM25° and WCOEE_20+DFM27° are found to be 0.014 g/kW.h; 0.021 g/kW.h; 0.019 g/kW.h; 0.016 g/kW.h and 0.018 g/kW.h which are found to be 26.32 %↓, 10.53 %↑, 0 % (same), 15.79 %↓, and 5.26 %↓ than diesel fuel (0.019 g/kW.h) respectively.

3.2.2. *Hydrocarbon emission (HC)*

The Fig. 6 illustrates the variation of unburned hydrocarbon (HC) emissions (in g/kW·h) as a function of brake power for six different fuel configurations in a single-cylinder VCR diesel engine operating under a constant speed of 1500 rpm, injection pressure of 240 bar, and compression ratio of 17.5:1. The fuel configurations include neat diesel, WCOEE_20 (20 % waste cooking oil ethyl ester blended with diesel), and four dual-fuel modes incorporating biogas with WCOEE_20 at different injection timings: 21°, 23°, 25°, and 27° before top dead center (bTDC), designated as WCOEE_20+DFM21°, DFM23°, DFM25°, and DFM27°, respectively. Hydrocarbon emissions are a direct indicator of incomplete combustion, often resulting from poor ignition quality, quenching effects, or insufficient oxidation in the combustion chamber [78]. At the lowest brake power of 1.28 kW, all fuel modes exhibit relatively high hydrocarbon emissions due to low cylinder temperatures and insufficient turbulence, which hinder complete combustion [79]. Diesel emits 0.056 g/kW·h of hydrocarbons with a corresponding EGT of 172.58 °C, while WCOEE_20 shows a slightly lower emission at 0.044 g/kW·h and a marginally higher EGT of 194.95 °C, owing to the oxygenated nature of the biodiesel enhancing [68,78]. In contrast, dual-fuel modes display higher HC emissions. WCOEE_20+DFM21° records the highest HC emission at 0.068 g/kW·h and the lowest EGT of 175.14 °C, owing to retarded injection timing that delays the ignition and increases fuel-air mixing difficulties, especially in low-load conditions [80]. Similarly, DFM23° and DFM27° produce 0.063 and 0.059 g/kW·h, respectively, indicating sub-optimal combustion. Among the dual-fuel modes, WCOEE_20+DFM25° yields the lowest HC emission (0.056 g/kW·h), implying that advanced injection timing improves combustion even at lower loads by facilitating better premixing and faster flame propagation [81,82]. As brake power increases to 2.56 kW, there is a marked reduction in hydrocarbon emissions across all fuel modes, driven by elevated in-cylinder temperatures and improved combustion kinetics [76]. Diesel's HC emission falls to 0.042 g/kW·h, and WCOEE_20 achieves 0.028 g/kW·h. The dual-fuel modes follow a similar trend with WCOEE_20+DFM21° still emitting the highest value at 0.049 g/kW·h, while DFM25° and DFM27° record comparatively lower values of 0.039 and 0.04 g/kW·h, respectively. This pattern highlights the influence of injection timing and charge preparation on ignition quality and oxidation behavior. Notably, WCOEE_20+DFM23° shows a modest reduction to 0.045 g/kW·h, indicating slightly improved combustion under this load. At medium load (3.84 kW), HC emissions continue to decline due to more efficient combustion facilitated by better atomization, turbulence, and increased residence time for fuel oxidation [83]. Diesel and WCOEE_20 emit 0.033 and 0.02 g/kW·h, respectively, whereas dual-fuel modes show values ranging between 0.026 and 0.035 g/kW·h. WCOEE_20+DFM25° remains among the lowest (0.029 g/kW·h), reinforcing the advantage of advanced injection in achieving more thorough combustion. Conversely, DFM23° exhibits the highest HC emission at this load (0.035 g/kW·h), possibly due to sub-optimal ignition delay and localized quenching [82]. At the highest brake power of 5.12 kW, the engine operates under optimal thermal conditions, resulting in further reductions in HC emissions. Diesel emits 0.025 g/kW·h, while WCOEE_20 achieves the lowest value at 0.013 g/kW·h, demonstrating the efficiency of biodiesel at full load. Among dual-fuel modes, WCOEE_20+DFM25° and DFM27° show competitive performance with emissions of 0.021 and 0.024 g/kW·h, respectively, attributed to advanced injection enhancing charge premixing and reducing ignition lag. However, DFM21° and DFM23° continue to exhibit slightly elevated emissions (0.03 and 0.026 g/kW·h), reaffirming the adverse effects of

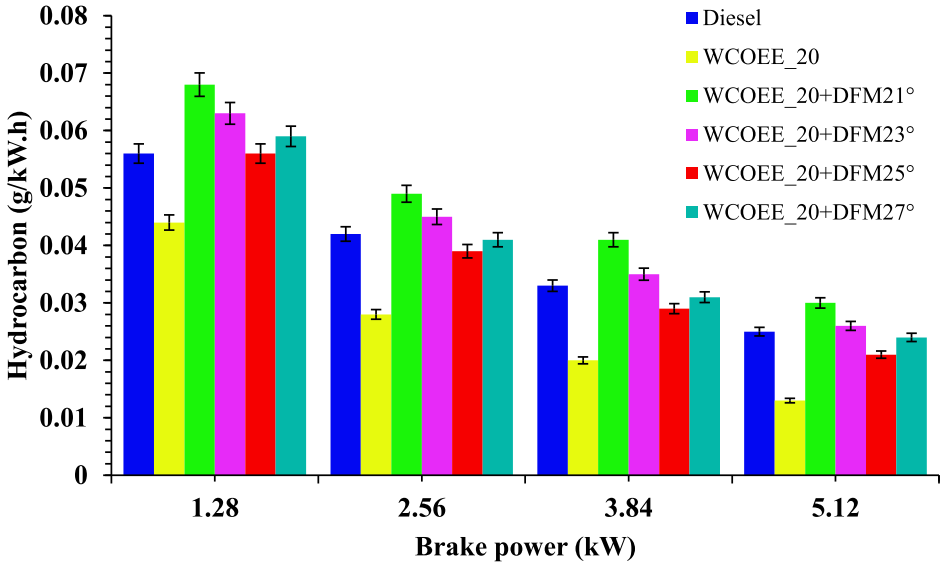

Fig. 6. Effect of test fuel blends with varying injector timing on HC (g/kW.h) vs. BP (kW).

retarded and standard timing under high-load conditions when the combustion duration becomes critical [84]. Thus, WCOEE_20+DFM25° shows the most favourable HC emission among the dual-fuel modes, particularly at higher loads, implying 25° bTDC as the best injection timing for biogas-inducted dual-fuel operation. The EGT trends across all conditions correlate strongly with the observed HC patterns, reinforcing the critical role of thermal energy in enabling complete combustion. These results align well with the findings of Ategle et al. [85], thereby validating the reliability of the adopted experimental approach. At peak load of 5.12 kW, HC emission values for WCOEE_20; WCOEE_20+DFM21°; WCOEE_20+DFM23°; WCOEE_20+DFM25° and WCOEE_20+DFM27° are found to be 0.013 g/kW.h; 0.03 g/kW.h; 0.026 g/kW.h; 0.021 g/kW.h and 0.024 g/kW.h which are found to be 48 %↓, 20 %↑, 4 %↑, 16 %↓, and 4 %↓ than diesel fuel (0.025 g/kW.h) respectively.

3.2.3. *Oxides of nitrogen*

Fig. 7 depicts the variation of nitrogen oxides (NOx) emissions (in g/kW·h) with respect to brake power for six different fuel configurations in a single-cylinder CI engine operating at a constant speed of 1500 rpm, injection pressure of 240 bar, and a compression ratio of 17.5:1. The fuel types considered include diesel, WCOEE_20 (20 % waste cooking oil ethyl ester blended with diesel), and four dual-fuel combinations incorporating biogas with WCOEE_20 under different injection timings: 21°, 23°, 25°, and 27° before top dead centre (bTDC), referred to respectively as WCOEE_20+DFM21°, DFM23°, DFM25°, and DFM27°. NOx formation is highly sensitive to combustion temperature and oxygen availability, primarily resulting from the thermal NO mechanism which becomes pronounced at high in-cylinder temperatures and prolonged residence times [86]. At low brake power (1.28 kW), diesel and WCOEE_20 exhibit the highest NOx emissions at 4.668 g/kW·h and 5.102 g/kW·h respectively. The higher value for WCOEE_20 can be attributed to its inherent oxygen content, which supports more complete combustion and raises peak flame temperatures, thereby promoting NOx formation [87,88]. The consistent reduction in both NOx and EGT in dual-fuel modes highlights biogas's role in lowering peak flame temperatures due to its high methane content and dilution effect, which suppress thermal NOx generation [89]. For instance, WCOEE_20+DFM21° emits only 3.326 g/kW·h, which further drops to 3.523, 3.641, and 3.74 g/kW·h for DFM23°, DFM25°, and DFM27° respectively. The lower NOx formation in these modes is due to the slower combustion of biogas and its lower adiabatic flame temperature, which reduces the peak in-cylinder temperature [90]. As the brake power increases to 2.56 kW, NOx emissions decrease slightly across all fuel types. Diesel drops to 3.582 g/kW·h and WCOEE_20 to 3.967 g/kW·h. Dual-fuel configurations continue to show reduced NOx levels, with WCOEE_20+DFM21° at 2.595 g/kW·h, DFM23° at 2.862 g/kW·h, DFM25° at 3.039 g/kW·h, and DFM27° at 3.318 g/kW·h. The reduction from 1.28 kW to 2.56 kW may be attributed to better charge homogeneity and shorter combustion duration, which limit the time available for NOx formation. The marginal increase in NOx and EGT in DFM27° suggests that overly advanced injection timing raises in-cylinder temperatures enough to partially negate biogas's cooling benefits [91]. At medium brake power (3.84 kW), NOx emissions further decline due to improved combustion efficiency and faster burning rates which reduce residence time at high temperatures [92]. Diesel records 2.961 g/kW·h and WCOEE_20 shows 3.296 g/kW·h. The dual-fuel modes maintain lower NOx emissions, with WCOEE_20+DFM21° and DFM23° dropping to 2.088 and 2.289 g/kW·h respectively, while DFM25° and DFM27° measure at 2.438 and 2.536 g/kW·h. These results highlight the effectiveness of biogas in mitigating NOx, especially when injection timing is optimized. Retarded timing (21° bTDC) significantly limits peak temperatures, thereby reducing NOx emissions the most. At full load (5.12 kW), diesel and WCOEE_20 continue their downward trend, recording NOx emissions of 2.467 g/kW·h and 2.793 g/kW·h respectively. The biogas-enriched dual-fuel modes show even lower values: 1.49 g/kW·h for WCOEE_20+DFM21, 1.865 for DFM23°, 2.043 for DFM25°, and 2.23 for DFM27°. The combination of biogas's low combustion temperature and the higher volumetric fuel consumption at full load helps suppress thermal NOx formation [93]. It is notable that as injection timing advances beyond 25° bTDC in dual fuel mode DFM25°, a slight rise in both NOx and EGT is observed, indicating that excessive advancement increases ignition pressure and peak temperature, partially offsetting biogas's cooling effect [90,93]. Thus, WCOEE_20+DFM21° shows the most favourable NOx emission among the dual-fuel modes, particularly at higher loads, implying retarded injection timing of 21° bTDC as the best injection timing for biogas-inducted dual-fuel operation. A marginal reduction in NO_x emissions was recorded under optimized injection timing, corroborating the findings of Raju et al. [94], who reported similar reductions when operating under leaner air-fuel mixtures and dual-fuel modes. At peak load of 5.12 kW, NOx emission values for WCOEE_20; WCOEE_20+DFM21°; WCOEE_20+DFM23°; WCOEE_20+DFM25° and WCOEE_20+DFM27° are found to be 2.79 g/kW.h; 1.49 g/kW.h; 1.86 g/kW.h; 2.04 g/kW.h and 2.23 g/kW.h which are found to be 12.96 % higher while, 39.68 %, 24.70 %, 17.41 %, and 9.72 % lower than diesel fuel (2.47 g/kW.h) respectively.

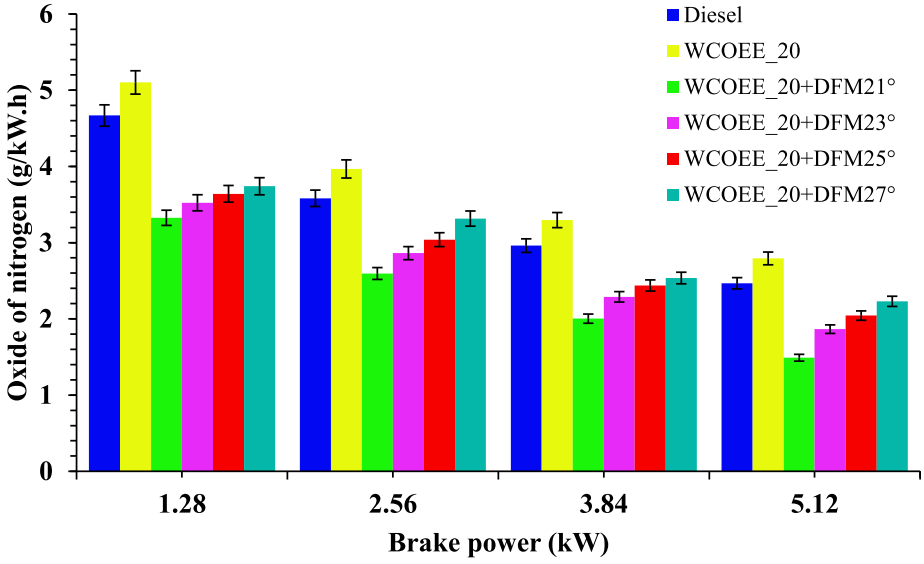

Fig. 7. Effect of test fuel blends with varying injector timing on NOx (g/kW.h) vs. BP (kW).

3.2.4. Smoke opacity

The Fig. 8 illustrates the variation of smoke opacity (%) with brake power for six fuel configurations in a compression ignition engine running at a constant speed of 1500 rpm, injection pressure of 240 bar, and a compression ratio of 17.5:1. The fuels examined include pure diesel, WCOEE_20 (a 20 % blend of waste cooking oil ethyl ester with diesel), and four dual-fuel variants combining WCOEE_20 with biogas at varying injection timings: WCOEE_20+DFM21, DFM23, DFM25, and DFM27, corresponding to 21°, 23°, 25°, and 27° before top dead center (bTDC), respectively. Smoke opacity serves as a measure of particulate matter (soot) concentration and is a key indicator of incomplete combustion, especially in diesel engines due to their diffusion flame characteristics [95]. At 0 kW brake power, the engine runs under no-load conditions, and diesel exhibits the highest smoke opacity at 7.89 %, reflecting its tendency for rich combustion and soot formation under cold conditions [96]. WCOEE_20 shows a slightly lower value at 6.67 %, attributable to the inherent oxygen content in biodiesel which promotes better combustion [88,89]. The dual-fuel configurations show further reductions, with values ranging from 5.94 % for DFM23° to 5.12 % for DFM25°. The presence of biogas, composed mainly of methane and carbon dioxide, helps in reducing localized fuel-rich zones and enhancing combustion homogeneity, thereby decreasing smoke emissions [97]. As brake power increases to 1.28 kW, smoke opacity rises for all fuels due to the increased fuel injection and combustion temperature, which enhances soot production [98]. Diesel reaches 12.55 %, while WCOEE_20 records 10.06 %. Dual-fuel modes maintain comparatively lower smoke values, ranging from 8.11 % (DFM25°) to 9.52 % (DFM21°). This trend indicates that biogas induction continues to play a key role in lowering particulate formation. Among the dual-fuel variants, WCOEE_20+DFM25° remains the most effective, possibly due to the optimal balance between oxygen availability and ignition timing that supports more complete combustion [98]. Moreover, the relatively higher EGT observed for DFM25° at this load (362.42 °C) compared to DFM21° (312.57 °C) implies more complete combustion and improved oxidation of soot particles. Higher exhaust gas temperatures facilitate post-flame soot oxidation, thus further contributing to the observed lower smoke opacity [90,94]. At 2.56 kW, the trend continues with diesel peaking at 18.71 % and WCOEE_20 at 15.09 %. In contrast, the dual-fuel combinations record values from 11.19 % to 13.27 %. Notably, the increase in smoke is relatively more subdued in the dual-fuel cases, further confirming biogas's influence in moderating rich zone combustion and improving oxidation of soot particles [99]. The lowest smoke opacity is again recorded with WCOEE_20+DFM25°, followed closely by DFM27°, implying that advancing injection timing in dual-fuel mode further enhances combustion phasing and soot oxidation [100]. This is further validated by the EGT trends at this load, where DFM25° recorded an EGT of 362.42 °C, suggesting more thorough combustion and more favorable thermal conditions for soot oxidation [98]. At higher loads of 3.84 kW and 5.12 kW, smoke opacity rises sharply for diesel and WCOEE_20, reaching 22.38 % and 18.85 % respectively at 3.84 kW, and 27.23 % and 24.74 % at full load. The high load conditions demand more fuel, leading to richer mixtures and thus greater soot formation [99,100]. The dual-fuel setups remain significantly cleaner, with WCOEE_20+DFM25° and DFM27° showing the lowest smoke opacity at these loads—12.14 % and 12.87 % at 3.84 kW, and 19.48 % and 21.03 % at 5.12 kW, respectively. The effectiveness of DFM25° and DFM27° at these loads may stem from more favorable in-cylinder conditions where advanced injection facilitates complete combustion before peak pressure, reducing the persistence of soot-producing zones [101,102]. Thus, WCOEE_20+DFM25° shows the most favourable smoke opacity emission reduction among the dual-fuel modes, particularly at higher loads, implying advanced injection timing of 25° bTDC as the best injection timing for biogas-inducted dual-fuel operation. The present study observed a reduction in smoke opacity during dual-fuel operation, consistent with Katuru et al. [62] who also attributed this to enhanced oxygen availability from biodiesel aiding better oxidation of soot precursors. At peak load of 5.12 kW, smoke opacity emission values for WCOEE_20; WCOEE_20+DFM21°; WCOEE_20+DFM23°; WCOEE_20+DFM25° and WCOEE_20+DFM27° are found to be 24.74 %, 21.83 %, 20.62 %, 19.48 % and 21.03 % which are found to be 9.18 %, 19.86 %, 24.30 %, 28.49 % and 22.80 % lower than diesel fuel (27.24 %) respectively.

3.3. Combustion characteristics

Combustion analysis in a diesel engine is crucial for evaluating the efficiency, stability, and effectiveness of the combustion process, which directly influences performance, and emissions. Key parameters studied includes heat release rate (HRR), in-cylinder pressure (CP), ignition delay period (IDP), and combustion duration (CD). HRR provides insight into how quickly and efficiently chemical energy from fuel is converted into thermal energy. CP measurements reflect the energy conversion process and combustion stability. Ignition delay period, the time between start of injection (SOI) and start of combustion (SOC), affects fuel-

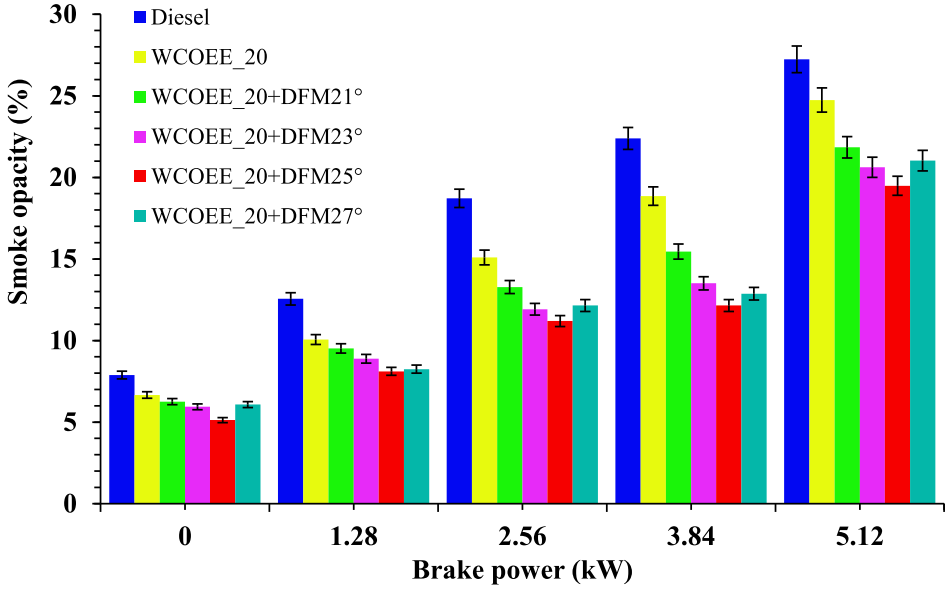

Fig. 8. Effect of test fuel blends with varying injector timing on smoke opacity (%) vs. BP (kW).

air mixing. CD, the time span over which most combustion occurs, impacts efficiency and emissions.

3.3.1. Heat release rate (HRR)

The Fig. 9 illustrates the heat release rate (HRR), expressed in Joules per degree crank angle (J/ °CA), plotted against crank angle (°CA) for various fuel types including diesel, WCOEE_20 (20 % waste cooking oil ethyl ester blended with diesel), and WCOEE_20 in dual-fuel mode with biogas at different injection timings—21°, 23°, 25°, and 27° before top dead center (bTDC). This analysis was performed at a constant engine speed of 1500 rpm, injection pressure of 240 bar, and a compression ratio of 17.5:1, with variable brake power ranging from 0 to 5.12 kW. The heat release rate is a vital combustion parameter that provides insights into the chemical energy release during the combustion process, influencing engine efficiency, pressure rise, and emission formation [103]. From the Fig. 9, the HRR curves for all fuel types exhibit a distinct double-peak profile. The first and more dominant peak corresponds to the premixed combustion phase, where accumulated fuel ignites rapidly after the ignition delay. The second, smaller peak is indicative of the diffusion-controlled combustion phase, where fuel burns as it is injected [99,103]. Diesel shows a sharp and high first peak just after top dead center (TDC), peaking 55.78 J/ °CA, reflecting its excellent atomization, volatility, and high cetane number that result in a shorter ignition delay and intense premixed combustion [104]. In comparison, WCOEE_20 also demonstrates a prominent premixed combustion peak of 52.37 J/ °CA, albeit slightly lower and shifted a few degrees later than diesel, due to the lower volatility and higher viscosity of biodiesel which leads to relatively longer ignition delay and slower fuel-air mixing [100]. The HRR peak of WCOEE_20 is marginally less intense, indicating smoother combustion with lower pressure rise rates. The dual-fuel configurations (WCOEE_20 + biogas) display noticeable deviations from the single-fuel profiles. For WCOEE_20+DFM21° (retarded injection at 21° bTDC), the premixed peak (50.43 J/ °CA) is notably lower and further delayed, reflecting a longer ignition delay period and reduced combustion intensity due to the lower reactivity of biogas, which has a high auto ignition temperature and low flame speed. This causes partial suppression of premixed combustion and a more gradual energy release [104]. As injection timing advances to 23° bTDC (DFM23°), the premixed peak becomes more pronounced and shifts slightly closer to TDC (52.84 J/ °CA), reflecting improved fuel-air mixing and earlier combustion onset. This trend continues with further advanced timings—25° (DFM25°) and 27° (DFM27°)—where the peak heat release increases slightly and occurs closer to TDC having values 54.73 J/ °CA and 53.99 J/ °CA. However, excessively advanced injection (27° bTDC) may lead to combustion occurring too early during the compression stroke, resulting in increased compression work and reduced thermal efficiency, as seen from the broader and flattened peak in the HRR curve [105]. Another crucial observation is the extended tail of the HRR curves in dual-fuel modes, particularly for DFM21° and DFM23°. This tail corresponds to the prolonged diffusion combustion phase, primarily due to the slower burning nature of biogas and possible incomplete combustion in quenching zones. The broader combustion duration for dual-fuel blends suggests a less efficient energy release, which may lead to higher unburned hydrocarbon emissions and lower thermal efficiency, particularly at higher biogas substitution ratios [104,106]. Quantitatively, while diesel and WCOEE_20 show heat release peaks of 55.78 J/ °CA and 52.37 J/ °CA respectively, dual-fuel blends range from approximately 50.43 to 54.73 J/ °CA in the premixed phase, with DFM21° on the lower end and DFM25° showing the highest HRR among dual-fuel modes. Thus, HRR curves affirm that diesel provides the most intense and immediate combustion, while WCOEE_20 yields a slightly delayed yet smoother heat release due to its oxygenated nature. Dual-fuel modes with biogas demonstrate moderated and extended combustion profiles, significantly influenced by injection timing. Advanced timings improve premixed combustion but risk early energy release losses, whereas retarded timings yield poor combustion efficiency due to delayed ignition and incomplete combustion [99,100]. Hence, WCOEE_20+DFM25° shows the most favourable heat release rate among the dual-fuel modes, implying advanced injection timing of 25° bTDC as the best injection timing for biogas-inducted dual-fuel operation. The HRR profile obtained in the current investigation closely resembles that of Yusuf et al. [107], showing a sharper and earlier peak under advanced injection timing due to improved premixed combustion. At peak load of 5.12 kW, HRR values for WCOEE_20; WCOEE_20+DFM21°; WCOEE_20+DFM23°; WCOEE_20+DFM25° and WCOEE_20+DFM27° are found to be 52.37, 50.43, 52.84, 54.73 and 53.99 J/ °CA which are found to be 6.11 %, 9.59 %, 5.27 %, 1.88 %, and 3.21 % lower than diesel fuel (55.78 J/ °CA) respectively.

3.3.2. In-cylinder pressure

In-cylinder pressure evaluation is an important diagnostic tool to comprehend the ignition operations that occur inside the engine's cylinders. The pressure measurement chart additionally offers information on the duration and extent of ignition, however it also has a direct

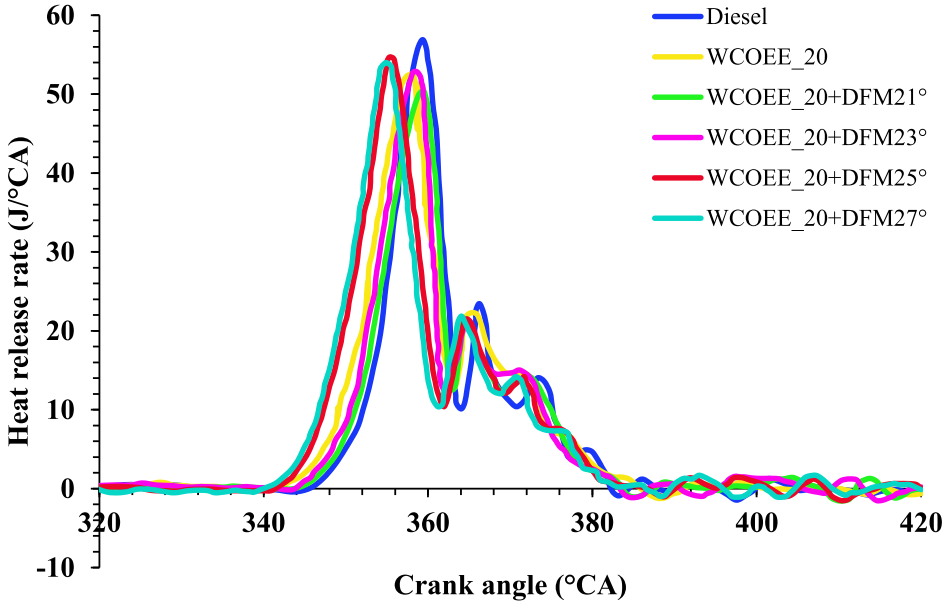

Fig. 9. Effect of test fuel blends with varying injector timing on HRR (J/°CA) vs. Crank angle (degree).

correlation to engine operation, combustion effectiveness, along with emissions. In-cylinder pressure measurements provide important information like start of combustion (SOC), peak cylinder pressure (PCP), rate of pressure rise (RoPR), and combustion duration (CD), each of these are essential for assessing the integrity and consistency of burning across various fueling conditions. Fig. 10 depicts the relationship between cylinder pressure alongside crank angle during maximum load circumstances considering three different modes of operation: normal diesel fuel, waste cooking oil ethyl ester (WCOEE), and biogas induced dual-fuel modes (BDFM) utilizing both advanced as well as retarded experimental fuel delivery injector timings (21 °CA; 23 °CA; 25 °CA; and 27 °CA bTDC). Diesel in single operational mode has a quick and swift increase in pressure because of its improved combustion properties including short ignition delay period (IDP) [108]. Since WCOEE has a greater kinematic viscosity along with less volatile characteristics than diesel fuel, the WCOEE_diesel blend has a somewhat retarded maximum pressure. The pilot injector timing influences the ignition morphology even more during biogas induced dual-fuel mode settings. Advanced injector timing serves to enhance ignition delay period (IDP), which causes a faster rate of pressure rise (RoPR), however retarded injector timing lowers peak pressure (PP). These changes have a significant impact on ignition stages, thermal performance, along with greenhouse gas emissions [109]. The in-cylinder pressure outlines produced with various fueling sources along with injector timing demonstrate the effect of ignition phase upon engine performance. The peak cylinder pressure (PCP) during standard diesel running remained about 73.5 bar, which occurred at 364.92 °CA. Powering with WCOEE_20 blend resulted in a somewhat reduced peak cylinder pressure of 67.61 bar at 364.94 °CA, probably because of variations in ignition characteristics alongside combustion reactivity [110]. Peak cylinder pressure and timings differed significantly whilst running in biogas induced dual-fuel modes (DFM) with different injector timings. Peak cylinder pressures (PCP) reported at injector timings of 21°, 23°, 25°, and 27°, seemed 65.05, 71.42, 80.86 and 75.41 bar, respectively, and occurred successively towards top dead centre (TDC) at 366.19°, 364.20°, 363.07°, and 363.17 °CA. These findings demonstrate that advancing the injector timing facilitates quicker and more intensive burning, boosting the maximum pressure and moving it towards TDC, indicating increased combustion performance [108]. At maximum workload, the WCOEE_20+DFM25° had an elevated peak cylinder pressure (PCP) over the WCOEE-diesel blend in single operational mode. This increase in PCP might be attributable towards the unique ignition kinetics induced during the dual-fuel approach. In DFM mode of operation, biogas—primarily methane along with carbon dioxide—is delivered via the inlet manifold, substituting some of the air being drawn in thereby lowering the amount of oxygen content inside the combustion zone. Since this reduction in concentration normally slows burning, the decreased responsiveness and more significant auto-ignition temperature of biogas lead the ignition delay period (IDP) to appear prolonged. A prolonged ignition delay period (IDP) allows for a greater formation of the pilot air-fuel mixtures until ignition occurs. As a consequence, whenever ignition takes place the built-up blended charge ignites quickly during the premixed combustible stage, resulting in a faster pressure rise eventually resulting in an enhanced peak cylinder pressure (PCP) [111,112]. The IT at 25 °CA bTDC looks to be appropriate in the current situation, enabling the pressure to accumulate around the top dead center (TDC). The pressure parameters seen in DFM25° operations are the result of a synergistic interactions involving extended ignition alongside quick premixed combustion. Results from experiments show that increasing the injector timing of WCOEE in dual-fuel running alongside biogas results in a significant rise in peak cylinder pressure (PCP). This increase in pressure is mostly due to the improved premixed ignition process linked to premature injections [112]. Whenever WCOEE injector timing advancement occurs, more fuel evaporate and blend into the ambient air along with induced biogas, yielding into a fuel-rich and uniformly distributed charges inside the combustion zone. When the piston reaches top dead center (TDC), the proficient combination burns quickly because it withstands the increased pressure and temperature circumstances associated with the premixed ignition stage. This causes an increased level of pressure rise because a large amount of the fuel spontaneously ignites promptly. As a result, the peak cylinder pressure (PCP) moves towards TDC, wherein the piston has the ideal location to use the expandable gases into mechanical work, enhancing its thermal performance [113]. Furthermore, premature combustion processes shorten the length of diffusion-controlled burning, resulting in shorter ignition periods as well as complete energy consumption before TDC. This cumulative impact reflects the increase in peak cylinder pressure (PCP) with advanced injector timing throughout dual-fuel operations. Thus, WCOEE_20+DFM25° shows the most favourable in-cylinder pressure among the dual-fuel modes, implying advanced injection timing of 25° bTDC as the best injection timing for biogas-inducted dual-fuel operation. Peak in-cylinder pressure was found to increase under dual-fuel operation, which aligns with the experimental trends reported by Raju et al. [94], suggesting improved combustion efficiency due to the high flame speed of the inducted gaseous fuel. At peak load of 5.12 kW, cylinder pressure values for WCOEE_20; WCOEE_20+DFM21°;

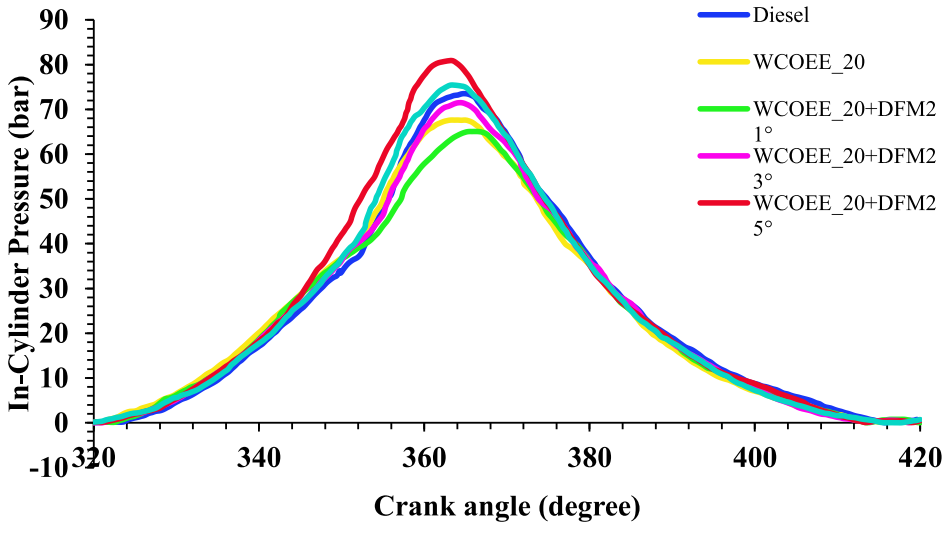

Fig. 10. Effect of test fuel blends with varying injector timing on ICP (bar) vs. Crank angle (degree).

WCOEE_20+DFM23°; WCOEE_20+DFM25° and WCOEE_20+DFM27° are found to be 67.61, 65.05, 71.42, 80.86 and 75.41 bar which are found to be 8.02 %, 11.05 %, and 2.83 %, lower while, 10.02 %, and 2.61 % higher than diesel fuel (73.5 bar) respectively.

3.3.3. Ignition delay period

The presented Fig. 11 illustrates the variation in ignition delay period (measured in degrees of crank angle, (°CA) with brake power for six different fuel configurations: pure diesel, WCOEE_20 (20 % waste cooking oil ethyl ester with diesel), and WCOEE_20 blended with biogas in a dual-fuel mode at different injection timings—DFM21°, DFM23°, DFM25°, and DFM27°—corresponding to 21°, 23°, 25°, and 27° before top dead centre (bTDC), respectively. The tests were conducted at a constant engine speed of 1500 rpm, injection pressure of 240 bar, and a compression ratio of 17.5:1. Ignition delay is defined as the interval between the start of injection and the beginning of combustion, and is a critical parameter affecting engine performance, combustion stability, and emissions [114]. At 0 kW brake power, which represents no-load or idling conditions, the ignition delay is longest across all fuel configurations. Diesel exhibits an ignition delay of 14.64 °CA, while WCOEE_20 shows a slightly shorter delay at 13.63 °CA due to its inherent oxygen content and higher cetane number, which support quicker ignition [103,105]. Among the dual-fuel combinations, WCOEE_20+DFM21° has the highest delay at 15.03 °CA, and the delay increases progressively with advanced injection timing, peaking at 16.84 °CA for WCOEE_20+DFM27°. The increase in ignition delay for dual-fuel modes at 0 kW is due to lower combustion chamber temperatures and the dilution effect of biogas, particularly methane, which has a high auto-ignition temperature and requires more energy to initiate combustion [115]. Advanced injection timing contributes further to this delay, as the injected fuel resides longer in a relatively colder cylinder environment before ignition. As the brake power increases to 1.28 kW, the ignition delay decreases for all fuel types due to higher cylinder pressures and temperatures, which accelerate the fuel-air mixture's ignition [111]. Diesel and WCOEE_20 show delays of 14.03 °CA and 12.73 °CA, respectively. Dual-fuel blends still display longer ignition delays compared to diesel and WCOEE_20, but there is a consistent reduction from their no-load values. WCOEE_20+DFM21° records 13.47 °CA, while DFM27° shows 14.81 °CA. The reduction in delay is influenced by the increase in in-cylinder thermal energy, which offsets the biogas's tendency to slow combustion. At 2.56 kW, a mid-load condition, the ignition delay continues to drop. Diesel and WCOEE_20 record delays of 12.87 °CA and 11.89 °CA, respectively. The dual-fuel configurations also exhibit reduced ignition delays, with WCOEE_20+DFM21° at 12.39 °CA, DFM23° at 12.51 °CA, DFM25° at 12.87 °CA, and DFM27° at 13.97 °CA. This downward trend indicates enhanced combustion kinetics due to rising in-cylinder temperatures, though biogas's influence remains evident in maintaining relatively longer delays in dual-fuel modes [116]. Interestingly, at this point, the differences among the dual-fuel timings begin to narrow, suggesting an increasingly favorable combustion environment. At 3.84 kW and 5.12 kW, corresponding to higher load conditions, the ignition delay values further decline, reaching their lowest across the operating range. Diesel achieves ignition delays of 12.04 °CA and 11.17 °CA, respectively, while WCOEE_20 shows even shorter delays of 11.03 °CA and 10.16 °CA. This further affirms the advantage of biodiesel's higher cetane number and oxygen content in enhancing ignition quality. In dual-fuel modes, delays fall to between 12.25 °CA (DFM25°) and 12.84 °CA (DFM27°) at 3.84 kW, and between 11.26 °CA (DFM27°) and 11.83 °CA (DFM23°) at 5.12 kW. Although ignition delays for dual-fuel modes remain slightly elevated compared to diesel and WCOEE_20, the gap narrows significantly at high loads due to increased combustion efficiency and higher thermal reactivity [115]. Overall, the ignition delay period (IDP) demonstrates an inverse relationship with brake power, as expected in internal combustion engines. The presence of biogas, with its slower burning characteristics and lower cetane behavior, inherently increases ignition delay, especially at lower loads. However, this effect is progressively counterbalanced by the rising in-cylinder temperatures at higher loads [116,117]. Among the injection timings, advanced timings such as DFM27° result in longer delays due to early fuel entry into cooler combustion chambers, while slightly advanced or standard timings like DFM23° and DFM25° offer a more balanced delay, suggesting more favorable conditions for dual-fuel combustion. Thus, WCOEE_20+DFM25° shows the most favourable ignition delay period among the dual-fuel modes, implying advanced injection timing of 25° bTDC as the best injection timing for biogas-inducted dual-fuel operation. The ignition delay period was extended under dual-fuel conditions, confirming the results by Yusuf et al. [57], which can be attributed to the higher auto-ignition temperature of biogas. At peak load of 5.12 kW, ignition delay period values for WCOEE_20; WCOEE_20+DFM21°; WCOEE_20+DFM23°; WCOEE_20+DFM25° and WCOEE_20+DFM27° are found to be 10.16 °CA, 10.93 °CA, 11.01 °CA, 11.26 °CA and 11.83 °CA which are found to be 9.04 %, 2.15 %, and 1.43 %, lower while, 0.83 %, and 5.91 % higher than diesel fuel (11.17 °CA) respectively.

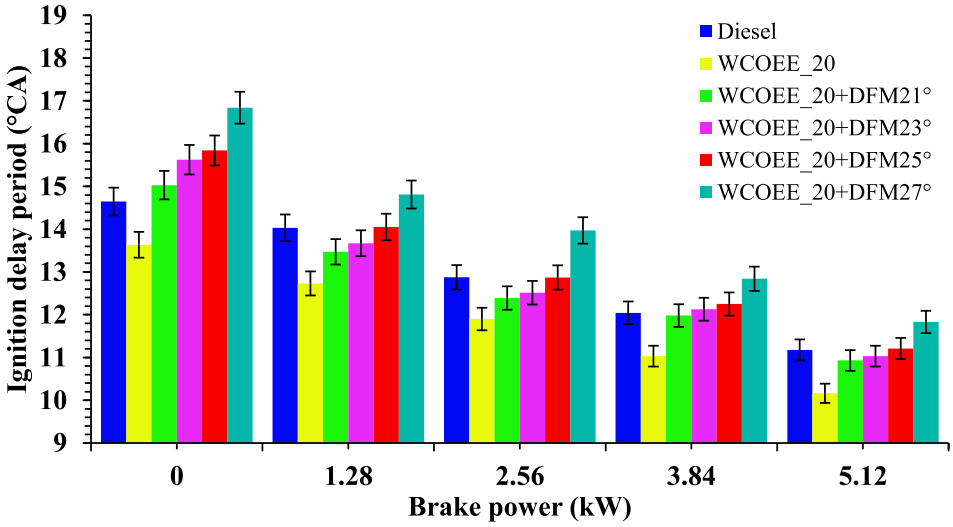

Fig. 11. Effect of test fuel blends with varying injector timing on IDP (°CA) vs. BP (kW).

3.3.4. Combustion duration

The Fig. 12 illustrates the variation in combustion duration, expressed in degrees of crank angle (°CA), with brake power for various fuel configurations—namely diesel, WCOEE_20 (20 % waste cooking oil ethyl ester with 80 % diesel), and WCOEE_20 blended with biogas under dual-fuel mode at different injection timings: 21° bTDC (WCOEE_20+DFM21), 23° bTDC (WCOEE_20+DFM23), 25° bTDC (WCOEE_20+DFM25), and 27° bTDC (WCOEE_20+DFM27). Experiments were carried out at a constant engine speed of 1500 rpm, injection pressure of 240 bar, and compression ratio of 17.5:1. Combustion duration refers to the total crank angle over which combustion occurs, from the start of ignition to the point where most of the fuel has been burned. This metric is crucial in determining engine efficiency, heat release rate, and emission characteristics. At no-load conditions (0 kW), diesel shows the shortest combustion duration at 24.34 °CA due to its favorable ignition properties and high cetane number that enable rapid combustion. WCOEE_20 exhibits a slightly longer duration at 25.28 °CA, which is attributed to its higher viscosity and oxygenated nature, resulting in slightly slower fuel atomization and flame propagation [112]. Dual-fuel configurations show progressively higher combustion duration with increasing injection timing. WCOEE_20+DFM21° records 26.22 °CA, and the values increase through WCOEE_20+DFM23° (26.05 °CA), WCOEE_20+DFM25° (25.37 °CA), reaching a maximum of 27.25 °CA for WCOEE_20+DFM27°. The prolonged duration in dual-fuel cases, especially with advanced injection timing, is mainly due to the presence of biogas—primarily methane—which has a lower flame speed and a higher ignition temperature, thus causing slower and more extended combustion [90,108]. As brake power increases to 1.28 kW, combustion duration increases for all fuel types due to greater fuel injection quantities and slower combustion of a denser fuel-air mixture. Diesel records 26.82 °CA, while WCOEE_20 shows 28.54 °CA. For dual-fuel blends, combustion duration rise sharply, with WCOEE_20+DFM21° at 30.34 °CA and WCOEE_20+DFM27° at 30.77 °CA. The increasing trend continues at 2.56 kW, where diesel records 31.11 °CA and WCOEE_20 registers 32.91 °CA. Combustion duration for dual-fuel blends span from 33.94 °CA (DFM21°) to 35.02 °CA (DFM27°), reflecting the increasing difficulty in rapidly burning biogas mixtures at moderate load, where biogas dilution effects are more prominent [111,118]. At 3.84 kW, the combustion duration further expands due to elevated fuel flow and slower combustion kinetics, especially under dual-fuel operation. Diesel's duration increases to 34.02 °CA and WCOEE_20 to 35.74 °CA. The dual-fuel blends show significantly higher combustion duration's, ranging from 37.31 °CA (DFM21°) to 37.714 °CA (DFM27°), with the highest values still associated with the most advanced injection timing. This reflects an extended combustion phase due to increased flame propagation delay in a biogas-rich, leaner mixture that burns more slowly compared to diesel. At the highest brake power of 5.12 kW, combustion duration reach their peak across all fuel types, as the combustion chamber conditions become increasingly demanding. Diesel records 36.85 °CA, and WCOEE_20 shows 38.91 °CA. The dual-fuel configurations exhibit combustion duration's ranging from 41.34 °CA (DFM21°) to 42.08 °CA (DFM27°). The further extension in combustion duration with dual-fuel blends and advanced injection timing is due to the compounded effects of larger fuel quantity, the slower-burning nature of biogas, and the early fuel entry which causes more heat loss before effective combustion begins [117]. The higher combustion duration in DFM27° also implies less efficient energy conversion and potentially higher emissions of unburned hydrocarbons due to incomplete combustion [107]. Thus, WCOEE_20+DFM25° shows the most favourable combustion duration among the dual-fuel modes, implying advanced injection timing of 25° bTDC as the best injection timing for biogas-inducted dual-fuel operation. The combustion duration was slightly prolonged in dual-fuel operation, which is consistent with Yusuf et al. [119], likely due to the lower flame propagation velocity of biogas. At peak load of 5.12 kW, combustion duration values for WCOEE_20; WCOEE_20+DFM21°; WCOEE_20+DFM23°; WCOEE_20+DFM25° and WCOEE_20+DFM27° are found to be 38.91 °CA, 41.31 °CA, 40.54 °CA, 39.42 °CA and 42.08 °CA which are found to be 5.59, 12.11 %, 10.02 %, 6.97 %, and 14.19 % lower than diesel fuel (36.85 °CA) respectively.

4. Conclusion and recommendation

Based on comprehensive experimental investigations, it is concluded that the dual-fuel mode utilizing 20 % waste cooking oil ethyl ester (WCOEE_20) with biogas induction and an optimized injection timing of 25° bTDC (WCOEE_20+DFM25°) yields the most promising results in terms of engine performance, combustion quality, and emission control. At full engine load (5.2 kW), this configuration delivered a 34.77 % increase in brake thermal efficiency (BTE) compared to conventional diesel, and a 9.51 % improvement over WCOEE_20+DFM23°, demonstrating enhanced combustion due to superior air-fuel mixing. In terms of fuel economy, brake specific fuel consumption (BSFC) was reduced by 11.05 % compared to WCOEE_20+DFM23°, though it remained higher than neat diesel. Emission analysis revealed a 19.26 % decrease in hydrocarbons (HC), 15.79 % decrease in carbon monoxide (CO), and 5.52 % reduction in smoke opacity relative to WCOEE_20+DFM23°,

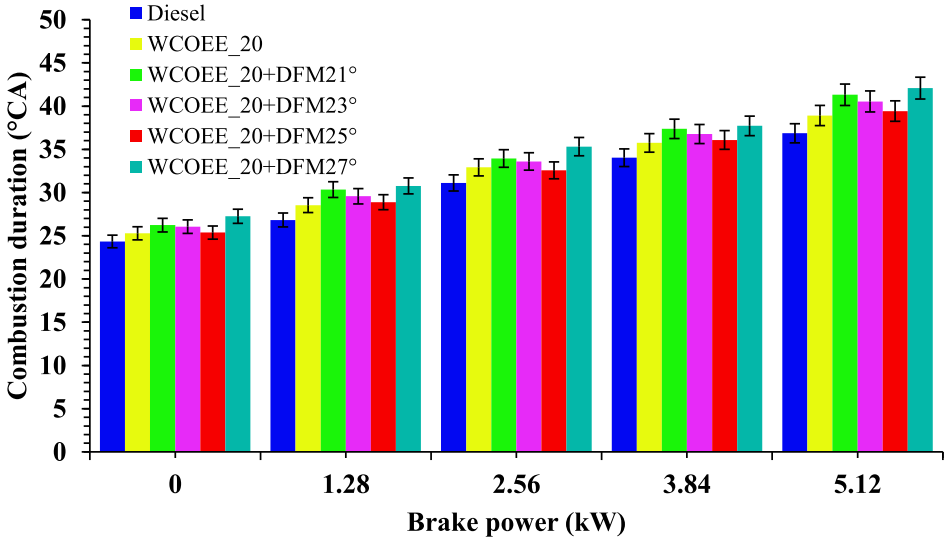

Fig. 12. Effect of test fuel blends with varying injector timing on CD (°CA) vs. BP (kW).

signifying cleaner combustion. However, a 9.67 % increase in NOx was observed, attributed to higher in-cylinder temperatures from advanced injection timing. Combustion analysis at WCOEE_20+DFM25° exhibited superior characteristics: peak in-cylinder pressure (CP) reached 80.86 bar, a 13.21 % increase over DFM23°; heat release rate (HRR) peaked at 54.73 J/ °CA, marking a 3.57 % rise; ignition delay period (IDP) increased by 2.27 %, and combustion duration (CD) shortened by 2.76 %, indicating faster and more controlled energy conversion. Overall, WCOEE_20+DFM25° represents the most optimal operational configuration tested, balancing thermal efficiency, emission reduction, and combustion stability. From these observations, the research concludes that WCOEE_20 is a viable alternative fuel and sustainable substitute for conventional fuel in modern diesel-powered vehicles. Among the test conditions, injector timing of 25° bTDC in dual-fuel mode (WCOEE_20+DFM25°) is recommended as best suited parametric modification because it offers the best compromise between efficient combustion, and smooth engine operation.

5. Scope of future research

For future work, it is recommended to explore further optimization strategies, including variable injection pressure, and split injection techniques, to better accommodate the slow burning nature of biogas. Additionally, real-time, combustion control system, could be developed to dynamically adjust injection timing based upon load and engine conditions, ensuring optimal performance under dual-fuel operation. Moreover, long-term durability tests and detailed emission studies should be conducted to fully understand the environmental benefits and mechanical implications of sustained operations on biodiesel-biogas dual-fuel systems.

CRediT authorship contribution statement

Prasant Kumar Patra: Resources, Project administration. **Swarup Kumar Nayak:** Resources, Project administration. **Purna Chandra Mishra:** Formal analysis, Data curation. **Ganesan Subbiah:** Methodology, Investigation, Funding acquisition. **Nandagopal Kaliappan:** Investigation, Funding acquisition. **Kamakshi Priya:** Supervision, Software.

Declaration of competing interest

The authors declare that they have no known competing financial interests or personal relationships that could have appeared to influence the work reported in this paper.

Acknowledgement

The authors would like to thank and extend their appreciation to School of Mechanical Engineering, Kalinga Institute of Industrial Technology (Deemed to be University) for providing the exceptional facilities, valuable support, setup available in I.C.Engine laboratory for carrying out the experimentation, and conducive environment that greatly contributed to the successful completion of the research work.

Data availability

No data was used for the research described in the article.

References

[1] X.P. Nguyen, A.T. Hoang, A.I. Ölçer, V.V. Pham, S.K. Nayak, Biomass-derived 2,5-dimethylfuran as a promising alternative fuel: an application review on the compression and spark ignition engine, Fuel Process. Technol. 214 (2021) 106687, https://doi.org/10.1016/j.fuproc.2020.106687.

[2] N. Bhanu Teja, Y. Devarajan, R. Mishra, S. Sivasaravanan, D. Thanikaivel Murugan, Detailed analysis on sterculia foetida kernel oil as renewable fuel in compression ignition engine, Biomass Convers. Biorefinery 13 (4) (2021) 2959–2970, https://doi.org/10.1007/s13399-021-01328-w.

[3] K.R. Mohanasundaram, N. Govindan, Effect of air preheating, exhaust gas recirculation, and hydrogen enrichment on biodiesel/methane dual fuel engine, Therm. Sci. 25 (2021) 449–464, https://doi.org/10.2298/TSCI191024146M.

[4] International Energy Agency (IEA), World Energy Outlook 2022, IEA, Paris, 2022. Available from: https://www.iea.org/reports/world-energy-outlook-2022.

[5] S.K. Nayak, P.C. Mishra, M.M. Noor, Simultaneous reduction of nitric oxide and smoke opacity in TDI dual fuel engine fuelled with calophyllum-diesel blends and waste wood chip gas for modified inlet valve and injector nozzle geometry, Energy 189 (2019) 116238, https://doi.org/10.1016/j.energy.2019.116238.

[6] R.V. Andrade, L.A.C. Castaneda, D.M.Y. Maya, P.S.P.C. Correa Junior, L.R. M. Pinto, E.E.S. Lora, et al., Assessment of laminar flame velocity of producer gas from biomass gasification using the Bunsen burner method, Int. J. Hydrogen. Energy 45 (2020) 11559–11568, https://doi.org/10.1016/j.ijhydene.2020.02.082.

[7] P. Sivamurugan, Y. Devarajan, Emission analysis of dual fuelled diesel engine, Int. J. Ambient Energy 42 (1) (2018) 15–17, https://doi.org/10.1080/01430750.2018.1517696.

[8] D. Tilman, J. Hill, C. Lehman, Carbon-negative biofuels from low-input high-diversity grassland biomass, Science 314 (5805) (2006) 1598–1600, https://doi.org/10.1126/science.1133306.

[9] H. Al Tanjil, Biogas as an alternative energy source in rural areas and public awareness: a case study in Jessore District, J. Energy Nat. Resour. 8 (2019), https://doi.org/10.11648/j.jenr.20190801.13.

[10] A. Sarkar, D. Sahu, D. Das, S.K. Nayak, B.K Mandal, Performance and emission study of ethanol-blended gasoline powered small VCR engine, Int. J. Energy Clean Environ. 23 (7) (2022) 1–12, https://doi.org/10.1615/InterJEnerCleanEnv.2021038246.

[11] V. Hariram, R. Sathishbabu, J. Godwin John, N. Kailiappan, K. Vijayakumar, E. Sangeeth Kumar, et al., Enhanced combustion and emission characteristics of diesel-algae biodiesel-hydrogen blends in a single-cylinder diesel engine, Results Eng. 26 (2025) 104676, https://doi.org/10.1016/j.rineng.2025.104676.

[12] J. Milano, M.Y. Ong, S.K. Tiong, F. Ideris, A.S. Silitonga, A.H. Sebayang, et al., A comparative study of the production of methyl esters from non-edible oils as potential feedstocks: process optimization and two-step biodiesel characterization, Results Eng. 25 (2025) 104285, https://doi.org/10.1016/j.rineng.2025.104285.

[13] V.V. Le, T.T. Huynh, A. Ölçer, S.K. Nayak, V.V. Pham, A remarkable review of the effect of lockdowns during COVID-19 pandemic on global PM emissions, Energy Sources Part A Recover. Util. Environ. Eff. (2020), https://doi.org/10.1080/15567036.2020.1853854.

[14] R. Sathyamurthy, D. Balaji, S. Gorjian, S.J. Muthiya, R. Bharathwaaj, S. Vasanthaseelan, et al., Performance, combustion and emission characteristics of a DI-CI diesel engine fueled with corn oil methyl ester biodiesel blends, Sustain. Energy Technol. Assess. 43 (2021) 100981, https://doi.org/10.1016/j.seta.2020.100981.

[15] U. Rajak, P. Nashine, T.K. Verma, Assessment of diesel engine performance using spirulina microalgae biodiesel, Energy 166 (2019) 1025–1036, https://doi.org/10.1016/j.energy.2018.10.098.

[16] S.K. Nayak, G.R. Behera, P.C. Mishra, S.K. Sahu, Biodiesel vs diesel: a race for the future, Energy Sources Part A Recover. Util. Environ. Eff. 39 (14) (2017) 1453–1460, https://doi.org/10.1080/15567036.2015.1062827.

[17] K. Kalaimurugan, S. Karthikeyan, M. Periyasamy, G.T. Mahendran, Dharmaprabhakaran. Performance, emission and combustion characteristics of RuO_2 nanoparticles addition with neochloris oleoabundans algae biodiesel on CI engine, Energy Sources Part A Recover. Util. Environ. Eff. 46 (2024) 4185–4199, https://doi.org/10.1080/15567036.2019.1694102.

[18] S. Gopa Kumar, A. Ramesh, Twin injector biogas diesel RCCI mode-an effective means to reduce NOx emissions without penalty in fuel consumption, Fuel 352 (2023) 129103, https://doi.org/10.1016/j.fuel.2023.129103.

[19] A. Ahmad, A.K. Yadav, S. Hasan, Biogas as a sustainable and viable alternative fuel for diesel engines: a comprehensive review of production, purification, economic analysis and performance evaluation, Proc. Inst. Mech. Eng. Part E J. Process. Mech. Eng. (2024), https://doi.org/10.1177/09544089241255930.

[20] A. Ahmad, A.K. Yadav, A. Singh, Predictive modeling and optimization of microalgae Chlorella vulgaris biodiesel production: assessing the performance of a raw biogas-powered diesel engine with diethyl ether blended biodiesel, J. Environ. Inform. 45 (1) (2025) 42–56, https://doi.org/10.3808/jei.202500531.

[21] A. Kumar, V.P. Singh, A. Srivastava, Sustainable biodiesel production via biotransesterification from inedible renewable oils using immobilized lipases from Candida rugosa, Results Eng. 25 (2025) 104358, https://doi.org/10.1016/j.rineng.2025.104358.

[22] N. Khatri, K.K. Khatri, Hydrogen enrichment on diesel engine with biogas in dual fuel mode, Int. J. Hydrogen. Energy 45 (11) (2020) 7128–7140, https://doi.org/10.1016/j.ijhydene.2019.12.167.

[23] V.N. Nguyen, B. Nayak, T.J. Singh, H.C. Le, X.P. Nguyen, Investigations on the performance, emission and combustion characteristics of a dual-fuel diesel engine fueled with induced bamboo leaf gaseous fuel and injected mixed biodiesel-diesel blends, Int. J. Hydrogen. Energy 54 (2024) 397–4177, https://doi.org/10.1016/j.ijhydene.2023.06.074.

[24] S. Madhu, G.M. Lionus Leo, P. Prathap, Y. Devarajan, R. Jayabal, Effective utilization of waste pork fat as a potential alternate fuel in CRDI research diesel engine – Waste reduction and consumption technique, Process. Saf. Environ. Prot. 172 (2023) 815–824, https://doi.org/10.1016/j.psep.2023.02.057.

[25] P.M. Rastogi, A. Sharma, N. Kumar, Effect of CuO nanoparticles concentration on the performance and emission characteristics of the diesel engine running on jojoba (Simmondsia chinensis) biodiesel, Fuel 286 (2021) 119358, https://doi.org/10.1016/j.fuel.2020.119358.
[26] P. Shrivastava, T.N. Verma, O.D. Samuel, A. Pugazhendhi, An experimental investigation on engine characteristics, cost and energy analysis of CI engine fuelled with Roselle, Karanja biodiesel and its blends, Fuel 275 (2020) 117891, https://doi.org/10.1016/j.fuel.2020.117891.
[27] S.K. Nayak, P.C. Mishra, S. Tripathy, Influence of compression ratio on combustion characteristics of a VCR engine using Calophyllum inophyllum biodiesel and diesel blends, J. Mech. Sci. Technol. 29 (9) (2015) 4047–4052, https://doi.org/10.1007/s12206-015-0850-2.
[28] J.B. Sajin, G.O. Pillai, M. Kesavapillai, S. Varghese, Effect of nanoparticle on emission and performance characteristics of biodiesel, Int. J. Ambient Energy 42 (2021), https://doi.org/10.1080/01430750.2019.1611650.
[29] D. Barik, A. Kumar, S. Murugan, Effect of compression ratio on combustion performance and emission characteristic of a direct injection diesel engine fueled with upgraded biogas-Karanja methyl ester-diethyl ether port injection, Energy Fuels 32 (2018) 5081–5089, https://doi.org/10.1021/acs.energyfuels.7b01977.
[30] D.C. Selvam, Y. Devarajan, Performance and emission analysis of Sterculia foetida biodiesel enhanced with butanol: combustion efficiency and emission mitigation, Results Eng. 25 (2025) 104586, https://doi.org/10.1016/j.rineng.2025.104586.
[31] R.A. Bakar, R. Widudo, K. Kadirgama, D. Ramasamy, T. Yusuf, M. K. Kamarulzaman, et al., Experimental analysis on the performance, combustion/emission characteristics of a DI diesel engine using hydrogen in dual fuel mode, Int. J. Hydrogen. Energy 52 (2024) 843–860, https://doi.org/10.1016/j.ijhydene.2022.04.129.
[32] H. Sharma, A. Dhir, S.K. Mahla, Application of clean gaseous fuels in compression ignition engine under dual fuel mode: a technical review and Indian perspective, J. Clean. Prod. 314 (2021) 128052, https://doi.org/10.1016/j.jclepro.2021.128052.
[33] P. APPAVU, Effect of injection timing on performance and emission characteristics of Palm biodiesel and Diesel blends, J. Oil Palm Res. (2018), https://doi.org/10.21894/jopr.2018.0057.
[34] M.F Al-Dawody, The effect of biogas and dimethyl ether on the thermal characteristics of a dual-fuel diesel engine: a numerical study, Biofuels Bioprod. Biorefin. 18 (1) (2023) 125–138, https://doi.org/10.1002/bbb.2553.
[35] S. Subramanian Jayagopal, E. Porpatham, S.K Arumugam, Experimental studies on the Jatropha-biogas dual fuel engine, Heat Transf. Eng. (2024), https://doi.org/10.1080/01457632.2024.2347175.
[36] S. Bhadra, H. Dewal, N. Kumar, Performance and emission characteristics analysis of LPGKaranja biodiesel on CI engine with optimization, Arab. J. Geosci. 16 (2023) 204, https://doi.org/10.1007/s12517-023-11299-z.
[37] T.A. Nguyen, T.Y. Pham, H.C. Le, V.G. Nguyen, L.H. Nguyen, Exploring the feasibility of dimethyl ether (DME) and LPG fuel blend for small diesel engine: a simulation perspective, Int. J. Renew. Energy Dev. 13 (3) (2024) 559–571, https://doi.org/10.61435/ijred.2024.60250.
[38] Meher et al., 2006 L.C. Meher, D. Vidya Sagar, S.N Naik, Technical aspects of biodiesel production by transesterification—a review, Renew. Sustain. Energy Rev. 10 (3) (2006) 248–268, https://doi.org/10.1016/j.rser.2004.09.002.
[39] D.Y.C. Leung, Y. Guo, Transesterification of neat and used frying oil: optimization for biodiesel production, Fuel Process Technol. 87 (10) (2006) 883–890, https://doi.org/10.1016/j.fuproc.2006.06.003.
[40] S.K. Nayak, G.R. Behera, P.C. Mishra, Exhaust from a dual-fuel engine using quinine nut oil and producer gas, Energy Sources Part A Recover. Util. Environ. Eff. 39 (2) (2017) 246–253, https://doi.org/10.1080/15567036.2015.1107863.
[41] S.K. Nayak, B. Nayak, P.C. Mishra, M.M. Noor, S. Nanda, Effects of biodiesel blends and producer gas flow on overall performance of a turbocharged direct injection dual-fuel engine, Energy Sources Part A Recover. Util. Environ. Eff. 46 (1) (2024) 4165–4184, https://doi.org/10.1080/15567036.2019.1694101.
[42] S.K. Nayak, P.C. Mishra, Emissions from sawdust biomass and diesel blends fuels, Energy Sources Part A Recover. Util. Environ. Eff. 38 (14) (2016) 2050–2057, https://doi.org/10.1080/15567036.2014.999177.
[43] G. Knothe, Dependence of biodiesel fuel properties on the structure of fatty acid alkyl esters, Fuel Process Technol. 86 (10) (2005) 1059–1070, https://doi.org/10.1016/j.fuproc.2004.11.002.
[44] Y.C. Sharma, B. Singh, Development of biodiesel: current scenario, Renew. Sustain. Energy Rev. 13 (6–7) (2009) 1646–1651, https://doi.org/10.1016/j.rser.2008.08.009.
[45] M. Canakci, J.H. Van Gerpen, Comparison of engine performance and emissions for petroleum diesel fuel, yellow grease biodiesel, and soybean oil biodiesel, Trans. ASAe 46 (4) (2003) 937–944, https://doi.org/10.13031/2013.13949.
[46] F. Monlau, C. Sambusiti, A. Barakat, M. Quéméneur, E. Trably, J.P. Steyer, H. Carrère, Inhibition effects of furanic and phenolic compounds from lignocellulosic and algal hydrolysates on anaerobic mixed cultures: a comprehensive review, Biotechnol. Adv. 32 (5) (2013) 934–951, https://doi.org/10.1016/j.biotechadv.2014.04.007.
[47] S. Dahiya, A.N. Kumar, J. Shanthi Sravan, S. Chatterjee, O. Sarkar, S.V. Mohan, Food waste biorefinery: sustainable strategy for circular bioeconomy, Bioresour. Technol. 248 (Pt A) (2018) 2–12, https://doi.org/10.1016/j.biortech.2017.07.176.
[48] P.K. Tiwari, S. Raj, S. Kumar, P. Singh, R. Swaraj, S. Sarkar, et al., Influence of calophyllum inophyllum and jojoba oil methyl ester blended with n-pentanol additive upon overall performance, combustion and emission characteristics of a TDI engine operated in natural aspirated mode, Fuel 288 (2021) 119576, https://doi.org/10.1016/j.fuel.2020.119576.
[49] G. Chembedu, P.V. Manu, Investigation of performance and emission of a diesel engine fuelled with preheated blends of diesel-watermelon seed biodiesel-isopentanol-turmeric oil, Process. Saf. Environ. Prot. 196 (2025) 106863, https://doi.org/10.1016/j.psep.2025.106863.
[50] B. Yang, L. Ning, B. Liu, G. Huang, Y. Cui, K. Zeng, Comparison study of particulate matter characteristics in a diesel/natural gas dual-fuel engine under different natural gas-air mixing operation conditions, Fuel 288 (2021) 119721, https://doi.org/10.1016/j.fuel.2020.119721.
[51] D.C. Selvam, Y. Devarajan, Evaluating the performance, combustion, and emission characteristics of decanol-enhanced Sterculia foetida biodiesel in diesel engines, Results. Eng. 26 (2025) 104936, https://doi.org/10.1016/j.rineng.2025.104936.
[52] V. Vasan, N.V. Sridharan, M. Feroskhan, S. Vaithiyanathan, B. Subramanian, P. C. Tsai, et al., Biogas production and its utilization in internal combustion engines: a review, Process. Saf. Environ. Prot. 186 (2024) 518–539, https://doi.org/10.1016/j.psep.2024.04.014.
[53] H. Ambarita, Internal combustion engine run on biogas is a potential solution to meet Indonesia emission target, IOP. Conf. Ser. Mater. Sci. Eng. 237 (2017) 012013, https://doi.org/10.1088/1757-899X/237/1/012013.
[54] H. Ambarita, Internal combustion engine run on biogas is a potential solution to meet Indonesia emission target, IOP. Conf. Ser. Mater. Sci. Eng. 237 (2017) 012013, https://doi.org/10.1088/1757-899X/237/1/012013.
[55] I. Amez, B. Castells, B. Llamas, D. Bolonio, M.J. García-Martínez, J.L. Lorenzo, et al., Experimental study of biogas–hydrogen mixtures combustion in conventional natural gas systems, Appl. Sci. 11 (2021) 6513, https://doi.org/10.3390/app11146513.
[56] S.K. Bisoi, K.B. Sahu, S.K. Nayak, P.C. Mishra, Influence of storage period on the thermal and oxidation stability of Jatropha biodiesel and their blends, Int. J. Mech. Eng. Technol. 9 (13) (2018) 918–927.
[57] A.A. Yusuf, H. Dandakouta, I. Yahuza, D.A. Yusuf, M.A. Mujtaba, A.S. El-Shafay, M.E.M. Soudagar, Effect of low CeO_2 nanoparticles dosage in biodiesel-blends on combustion parameters and toxic pollutants from common-rail diesel engine, Atmos. Pollut. Res. 13 (2) (2022) 101305, https://doi.org/10.1016/j.apr.2021.101305.
[58] T.Z. Ang, M. Salem, M. Kamarol, H.S. Das, M.A. Nazari, N. Prabaharan, A comprehensive study of renewable energy sources: classifications, challenges and suggestions, Energy Strat. Rev. 43 (2022) 100939, https://doi.org/10.1016/j.esr.2022.100939.
[59] Y. Rajesh, A. Kolakoti, B. Sheakar, J. Bhargavi, Optimization of biodiesel production from waste frying palm oil using definitive screening design, Int. J. Eng. Sci. Technol. 11 (2) (2019) 48–57, https://doi.org/10.4314/ijest.v11i2.4.
[60] S.K. Nayak, G.R. Behera, P.C. Mishra, Physio-chemical characteristics of Punnang oil and rice husk-generated producer gas, Energy Sources Part A Recover. Util. Environ. Eff. 39 (3) (2017) 291–298, https://doi.org/10.1080/15567036.2015.1065297.
[61] G.M. Pinto, R.B.R. da Costa, T.A.Z. de Souza, A.J.A.C. Rosa, O.O. Raats, L.F. A. Roque, et al., Experimental investigation of performance and emissions of a CI engine operating with HVO and farnesane in dual-fuel mode with natural gas and biogas, Energy 277 (2023) 127648, https://doi.org/10.1016/j.energy.2023.127648.
[62] B.K. Prasad, V.D. Raju, A.A. Shaik, R.K. Gopidesi, M.B.S. Reddy, M.E. M. Soudagar, M.A. Mujtaba, Impact of injection timings and exhaust gas recirculation rates on the characteristics of diesel engine operated with neat tamarind biodiesel, Energy Sources Part A 47 (1) (2021) 7767–7785, https://doi.org/10.1080/15567036.2021.1924314.
[63] N.M. Kumar, H. Bhavsar, G. Sakthivel, M.M. Feroskhan, K. Karunamurthy, Performance and emission characteristics of dual fuel engine using biodiesels, IOP. Conf. Ser. Earth. Environ. Sci. 850 (1) (2021) 012005, https://doi.org/10.1088/1755-1315/850/1/012005.
[64] H. Ambarita, Performance and emission characteristics of a small diesel engine run in dual-fuel (diesel-biogas) mode, Case Stud. Therm. Eng. 10 (2017) 179–191, https://doi.org/10.1016/j.csite.2017.06.003.
[65] D.C. Selvam, Y. Devarajan, T. Raja, Characterization of isopropanol-enhanced Caesalpinia bonduc biodiesel blends: a sustainable strategy for decarbonization, Results. Eng. 25 (2025) 103849, https://doi.org/10.1016/j.rineng.2024.103849.
[66] D.K. Ramesha, A.S. Bangari, C.P. Rathod, R. Samartha Chaitanya, Experimental investigation of biogas-biodiesel dual fuel combustion in a diesel engine, Mech. Eng. Sci. J. (2015) 12–20, https://doi.org/10.1515/mecdc-2015-0003.
[67] S.K. Bisoi, S.K. Nayak, K.B. Sahu, P.C. Mishra, Experimental evaluation on Jatropha biodiesel blends as an alternative fuel for engine application, Int. J. Mech. Eng. Technol. 8 (8) (2017) 1254–1262.
[68] P. Rosha, A. Dhir, S. Mohapatra, Influence of gaseous fuel induction on the various engine characteristics of a dual fuel compression ignition engine: a review, Renew. Sustain. Energy Rev. 82 (3) (2018) 3333–3349, https://doi.org/10.1016/j.rser.2017.10.055.
[69] H.N. Singh, A. Layek, Experimental study of the effect of compression ratio on the characteristics of a biogas fueled dual fuel compression ignition engine, Int. J. Renew. Energy Res. 8 (4) (2018) 2075–2084.
[70] G. Goga, B.S. Chauhan, S.K. Mahla, A. Dhir, H.M. Cho, Combined impact of varying biogas mass flow rate and rice bran methyl esters blended with diesel on a dual-fuel engine, Energy Sources Part A Recover. Util. Environ. Eff. 43 (1) (2019) 120–132, https://doi.org/10.1080/15567036.2019.1623948.
[71] M. Marikatti, N.R. Banapurmath, V.S. Yaliwal, Y.H. Basavarajappa, M.E. M. Soudagar, F.P.G. Márquez, M. Mujtaba, H. Fayaz, B. Naik, T.M.Y. Khan, A. Afzal, A.I. EL-Seesy, Hydrogen injection in a dual fuel engine fueled with low-pressure injection of methyl ester of Thevetia peruviana (METP) for diesel engine

maintenance application, Energies 13 (21) (2020) 5663, https://doi.org/10.3390/en13215663.
[72] M.M. Ibrahim, J.V. Narasimhan, A. Ramesh, Comparison of the predominantly premixed charge compression ignition and the dual fuel modes of operation with biogas and diesel as fuels, Energy 89 (2015) 990–1000, https://doi.org/10.1016/j.energy.2015.06.033.
[73] B.J. Bora, U.K. Saha, Estimating the theoretical performance limits of a biogas powered dual fuel diesel engine using emulsified rice bran biodiesel as pilot fuel, J. Energy Resour. Technol. 138 (2) (2016) 021801, https://doi.org/10.1115/1.4031836.
[74] S. Vellaiyan, Optimization of Spirulina biodiesel-ammonium hydroxide blends with exhaust gas recirculation for enhanced diesel engine performance and emission reduction, Results Eng. 26 (2025) 105015, https://doi.org/10.1016/j.rineng.2025.105015.
[75] G. Varghese, K. Saeed, X. Lu, K.J. Rutt, Measurements of the tailpipe emissions characteristics of algae biodiesel compared with the 1st and 2nd generation biodiesel fuels, Fuel 388 (2025) 134315, https://doi.org/10.1016/j.fuel.2025.134315.
[76] C. Deheri, S.K. Acharya, D.N. Thatoi, A.P Mohanty, A review on performance of biogas and hydrogen on diesel engine in dual fuel mode, Fuel 260 (2020) 116337, https://doi.org/10.1016/j.fuel.2019.116337.
[77] S.R. Reddy, G. Murali, A.A. Shaik, V.D. Raju, M.B.S. Reddy, Experimental evaluation of diesel engine powered with waste mango seed biodiesel at different injection timings and EGR rates, Fuel 285 (2021) 119047, https://doi.org/10.1016/j.fuel.2020.119047.
[78] R. Bouguessa, L. Tarabet, K. Loubar, T. Belmrabet, M. Tazerout, Experimental investigation on biogas enrichment with hydrogen for improving the combustion in diesel engine operating under dual fuel mode, Int. J. Hydrogen. Energy 45 (15) (2020) 9052–9063, https://doi.org/10.1016/j.ijhydene.2020.01.003.
[79] M.G. Leykun, M.W. Mekonen, Investigation of the performance and emission characteristics of diesel engine fueled with biogas-diesel dual fuel, Fuels 3 (1) (2022) 15–30, https://doi.org/10.3390/fuels3010002.
[80] A. Ahmad, A.K. Yadav, A. Singh, Process optimization of spirulina microalgae biodiesel synthesis using RSM coupled GA technique: a performance study of a biogas-powered dual-fuel engine, Int. J. Environ. Sci. Technol. 21 (2024) 169–188, https://doi.org/10.1007/s13762-023-04948-z.
[81] M. Bembenek, V. Melnyk, B. Karwat, T. Rokita, M. Hnyp, Y. Mosora, Ł. Warguła, Study of the technical and operational parameters of injectors using biogas fuel, Energies 17 (21) (2024) 5445, https://doi.org/10.3390/en17215445.
[82] S.K. Nayak, P.C. Mishra, Emission characteristics of jatropha oil blends using waste wood producer gas, Energy Sources Part A Recover. Util. Environ. Eff. 38 (14) (2016) 2153–2160, https://doi.org/10.1080/15567036.2014.989340.
[83] A. Rimkus, S. Stravinskas, J. Matijošius, J. Hunicz, Effects of different gas energy shares on combustion and emission characteristics of compression ignition engine fueled with dual-fossil fuel and dual-biofuel, Energy 312 (2024) 133443, https://doi.org/10.1016/j.energy.2024.133443.
[84] A. Sharma, N.A. Ansari, A. Pal, Y. Singh, S. Lalhriatpuia, Effect of biogas on the performance and emissions of diesel engine fuelled with biodiesel-ethanol blends through response surface methodology approach, Renew. Energy 141 (2019) 657–668, https://doi.org/10.1016/j.renene.2019.04.031.
[85] M.R. Atelge, E. Arslan, D. Krisa, R.R. Al-Samaraae, S. Abut, S. Ünalan, A. E. Atabani, N. Kahraman, S.O. Akansu, M. Kaya, S. Sarıkoç, H.D. Kıvrak, Comparative investigation of multi-walled carbon nanotube modified diesel fuel and biogas in dual fuel mode on combustion, performance, and emission characteristics, Fuel 313 (2022) 123008, https://doi.org/10.1016/j.fuel.2021.123008.
[86] S.S. Kalsi, K.A. Subramanian, Effect of simulated biogas on performance, combustion and emissions characteristics of a biodiesel fueled diesel engine, Renew. Energy 106 (2017) 78–90, https://doi.org/10.1016/j.renene.2017.01.006.
[87] S.K. Nayak, P.C. Mishra, G.R. Behera, Experimental investigation on dual-fuel engine utilizing waste cooking oil and producer gas, Energy Sources Part A Recover. Util. Environ. Eff. 39 (4) (2017) 369–376, https://doi.org/10.1080/15567036.2015.1122684.
[88] K.A. Rahman, A. Ramesh, Studies on the effects of methane fraction and injection strategies in a biogas diesel common rail dual fuel engine, Fuel 236 (2019) 147–165, https://doi.org/10.1016/j.fuel.2018.08.091.
[89] A. Sharma, Y. Singh, N.A. Ansari, A. Pal, S. Lalhriatpuia, Experimental investigation of the behaviour of a DI diesel engine fuelled with biodiesel/diesel blends having effect of raw biogas at different operating responses, Fuel 279 (2020) 118460, https://doi.org/10.1016/j.fuel.2020.118460.
[90] B.J. Bora, U.K. Saha, S. Chatterjee, V. Veer, Effect of compression ratio on performance, combustion and emission characteristics of a dual fuel diesel engine run on raw biogas, Energy Convers. Manage 87 (2014) 1000–1009, https://doi.org/10.1016/j.enconman.2014.07.080.
[91] H. Yaqoob, H.M. Ali, U. Sajjad, K. Hamid, Investigating the potential of plastic pyrolysis oil-diesel blends in diesel engine: performance, emissions, thermodynamics and sustainability analysis, Results. Eng. 24 (2024) 103336, https://doi.org/10.1016/j.rineng.2024.103336.
[92] M. Govindasamy, M. Ezhumalai, A. Munimathan, S. Dixit, S. Singh, R. Dhairiyasamy, Lemongrass oil as a renewable additive for enhancing the oxidation and thermal properties of Calophyllum Inophyllum biodiesel, Results. Eng. (2025) 105102, https://doi.org/10.1016/j.rineng.2025.105102.
[93] E.V. Geo, C. Prabhu, S. Thiyagarajan, T. Maiyalagan, F. Aloui, Comparative analysis of various techniques to improve the performance of novel wheat germ oil – An experimental study, Int. J. Hydrogen. Energy 45 (9) (2020) 5745–5756, https://doi.org/10.1016/j.ijhydene.2019.05.198.
[94] V.D. Raju, J.N. Nair, H. Venu, L. Subramani, M.E.M. Soudagar, M.A. Mujtaba, T. M.Y. Khan, et al., Combined assessment of injection timing and exhaust gas recirculation strategy on the performance, emission and combustion characteristics of algae biodiesel powered diesel engine, Energy Sources Part A 44 (4) (2022) 8554–8571, https://doi.org/10.1080/15567036.2022.2123068.
[95] S.K. Nayak, P.C. Mishra, A. Kumar, G.R. Behera, B. Nayak, Experimental investigation on property analysis of Karanja oil methyl ester for vehicular usage, Energy Sources Part A Recover. Util. Environ. Eff. 39 (3) (2017) 306–312, https://doi.org/10.1080/15567036.2016.1173131.
[96] A.R. Adib, M.M. Rahman, T. Hassan, A. Ahmed, A.A. Rifat, Novel biofuel blends for diesel engines: optimizing engine performance and emissions with C. cohnii microalgae biodiesel and algae-derived renewable diesel blends, Energy Convers. Manag.:X 23 (2024) 100688, https://doi.org/10.1016/j.ecmx.2024.100688.
[97] S.S. Halewadimath, N.R. Banapurmath, V.S. Yaliwal, M.G. Prasad, S.S. Jalihal, M. E.M. Soudagar, et al., Effect of manifold injection of hydrogen gas in producer gas and neem biodiesel fueled CRDI dual fuel engine, Int. J. Hydrogen. Energy 47 (2022) 25913–25928, https://doi.org/10.1016/j.ijhydene.2022.02.135.
[98] S.K. Dash, P. Lingfa, D. Barik, Combined adjustment of injection timing and compression ratio for an agricultural diesel engine fuelled with Nahar methyl ester, Int J Ambient Energy 43 (1) (2022) 1482–1494, https://doi.org/10.1080/01430750.2020.1712250.
[99] E. Tomita, N. Kawahara, U. Azimov, Combustion and exhaust emissions of biogas dual-fuel engines, SpringerBriefs Appl. Sci. Technol. (2022) 43–72, https://doi.org/10.1007/978-3-030-94538-1_3.
[100] S.K. Nayak, P.C. Mishra, A. Kumar, G.R. Behera, Characterization of coconut shell imitated producer gas in a diesel engine, Energy Sources Part A Recover. Util. Environ. Eff. 39 (16) (2017) 1718–1724, https://doi.org/10.1080/15567036.2016.1141266.
[101] T.I. Kasih, Y. Oishi, D. Ogawa, H. Kawai, H. Ambarita, Determination of the optimum biogas energy ratio in dual-fuel biodiesel used in cooking oil-biogas operation, Energy Sources, Part A: Recover., Utiliz. Environ. Eff. 45 (4) (2023) 13001–13020, https://doi.org/10.1080/15567036.2023.2278725.
[102] P. Sharma, B.B. Sahoo, Z. Said, H. Hadiyanto, X.P. Nguyen, S. Nizetic, Z. Huang, A.T. Hoang, C. Li, Application of machine learning and Box-Behnken design in optimizing engine characteristics operated with a dual-fuel mode of algal biodiesel and waste-derived biogas, Int. J. Hydrogen. Energy 48 (18) (2023) 6738–6760, https://doi.org/10.1016/j.ijhydene.2022.04.152.
[103] B.B. Kishore, G.N. Kumar, Effect of fuel injection timing on engine characteristics with an equal volume of 1-heptanol/diesel blend in a CRDI CI engine, Results. Eng. 26 (2025) 104632, https://doi.org/10.1016/j.rineng.2025.104632.
[104] S.K. Nayak, D.B. Munuswamy, G. Subbiah, M. Naresh, Y. Devarajan, Influence of diglyme and cumene additives upon emission and combustion behaviour of diverse biodiesel fuelled diesel engine, Results. Eng. 25 (2025) 104255, https://doi.org/10.1016/j.rineng.2025.104255.
[105] S.K. Mahla, S.M.S. Ardebili, M. Rabeti, G. Goga, A. Dhir, H. Sharma, Performance and exhaust emissions analysis of a diesel engine running on diesel/diethyl ether/biogas as a green fuel, Energy Sources, Part A: Recover., Utiliz. Environ. Eff. 44 (4) (2022) 9395–9411, https://doi.org/10.1080/15567036.2022.2133194.
[106] C.K. Nayak, B.P. Pattanaik, J.K. Panda, Trade-off study on economy and environmental aspects of a dual-fuel diesel engine using diesel additive and producer gas, J. Energy Resour. Technol., Trans. ASME 144 (3) (2022) 032306, https://doi.org/10.1115/1.4052862.
[107] A.A. Yusuf, J.D. Ampah, I. Veza, A.E. Atabani, A.T. Hoang, A. Nippae, M. T. Powoe, S. Afrane, D.A. Yusuf, I. Yahuza, Investigating the influence of plastic waste oils and acetone blends on diesel engine combustion, pollutants, morphological and size particles: dehalogenation and catalytic pyrolysis of plastic waste, Energy Convers. Manage 291 (2023) 117312, https://doi.org/10.1016/j.enconman.2023.117312.
[108] K.M. Gowthama, S. Rajkumar, Effects of start of injection and exhaust gas recirculation on dual fuel combustion of isobutanol with diesel and waste cooking oil biodiesel in a diesel engine at higher loads, Fuel 327 (2022) 125097, https://doi.org/10.1016/j.fuel.2022.125097.
[109] S.K. Mahla, G. Goga, H.M. Cho, A. Dhir, B.P. Chauhan, Separate effect of biodiesel, n-butanol, and biogas on performance and emission characteristics of diesel engine: a review, Biomass Convers. Biorefinery 13 (1) (2023) 447–469, https://doi.org/10.1007/s13399-020-01056-7.
[110] P. Kumar, P.M.V. Subbarao, V.K. Vijay, S.A. Khan, A. Sharma, L.D. Kala, Performance assessment of compression ignition engines powered by biogas, biodiesel, and producer gas mix derived from agriculture waste, Biofuels 14 (9) (2023) 921–931, https://doi.org/10.1080/17597269.2023.2190574.
[111] Khairil, M. Syaukani, S. Bahri, S.E. Sofyan, A.Z. Mubarak, Ali M Zulfadhli, Experimental study the effect of using fuels from pyrolysis of waste tire oil-diesel blends on the CI-engine performance, Results. Eng. 26 (2025) 104701, https://doi.org/10.1016/j.rineng.2025.104701.
[112] A. Mohite, B.J. Bora, P. Sharma, S. Sendemir, D. Mallick, S. Sunil, U. Agbulut, Performance enhancement and emission control through adjustment of operating parameters of a biogas-biodiesel dual fuel diesel engine: an experimental and statistical study with biogas as a hydrogen carrier, Int. J. Hydrogen. Energy 52 (2024) 752–764, https://doi.org/10.1016/j.ijhydene.2023.08.201.
[113] C. Thiagarajan, M. Prabhahar, S. Prakash, M. Karthick Raja, D. Kumar, A. Thangapandiyan, Performance and emissions characteristics of algae oil methyl ester with different methanol injection positions in dual-fuel engine, Springer Proc. Mater. 58 (2024) 295–303, https://doi.org/10.1007/978-981-97-6875-2_31.

[114] M.C. Barot, P.R. Shah, D.R. Shah, N.K. Shah, A.H. Kolekar, Experimental investigation of biogas and Karanja biodiesel blend on the effect of performance and emissions of dual-fuel C.I. Engine, in: Green Energy and Technology, ICAER 2023, Mumbai, 2024, pp. 285–303, https://doi.org/10.1007/978-981-97-5419-9_25.

[115] R.K. Mohan, J. Sarojini, U. Agbulut, U. Rajak, T.N. Verma, K.T. Reddy, Energy recovery from waste plastic oils as an alternative fuel source and comparative assessment of engine characteristics at varying fuel injection timings, Energy 275 (2023) 127374, https://doi.org/10.1016/j.energy.2023.127374.

[116] V.N. Nguyen, S.K. Nayak, H.S. Le, J. Kowalski, D. Balakrishna, D. Xuan Quang, T. Thanh Hai, T. Viet Duang, D.N. Cao, P.Q.P. Nguyen, Performance and emission characteristics of diesel engines running on gaseous fuels in dual-fuel mode, Int. J. Hydrogen. Energy 49 (2024) 868–909, https://doi.org/10.1016/j.ijhydene.2023.09.130.

[117] N. Khayum, A. Subramanian, S. Murugan, Effect of nozzle opening pressure on combustion, performance, and emission analyses of a dual fuel diesel engine, Energy Sources, Part A: Recover., Utiliz. Environ. Eff. 46 (1) (2024) 10121–10140, https://doi.org/10.1080/15567036.2020.1780349.

[118] S. Ravishankar, Performance and emission characteristics of fish oil methyl ester in direct injection diesel engine with hydrogen enrichment - an experimental approach, Results. Eng. 26 (2025) 104983, https://doi.org/10.1016/j.rineng.2025.104983.

[119] A.A. Yusuf, I. Veza, J.D. Ampah, S. Afrane, S. Sarikoç, M.A. Mujtaba, I. Yahuza, Experimental study on emissions and particulate characteristics of diesel engine fueled with plastic waste oil, acetone-butanol-ethanol and diesel blends, Process. Saf. Environ. Prot. 191 (Pt A) (2024) 1419–1431, https://doi.org/10.1016/j.psep.2024.09.060.